8021219

FABISIAK, WALTER

CORRELATION OF THIXOTROPIC PARAMETERS AND RELATED TESTS OF BLOOD FROM HUMAN SUBJECTS

New Jersey Institute of Technology D.ENG.SC. 1980

University Microfilms International 300 N. Zeeb Road, Ann Arbor, MI 48106 18 Bedford Row, London WC1R 4EJ, England

CORRELATION OF THIXOTROPIC PARAMETERS AND RELATED TESTS OF BLOOD FROM HUMAN SUBJECTS

by

Walter Fabisiak

Dissertation submitted to the Faculty of the Graduate School of the New Jersey Institute of Technology in partial fulfillment of the requirements for the degree of Doctor of Engineering Science

1980

APPROVAL SHEET

Title of Thesis: Correlation of Thixotropic Parameters and Related Tests of Blood From Human Subjects

Name of Candidate: Walter Fabisiak
Doctor of Engineering Science, 1980

Thesis and Abstract Approved: ______________________

Ching-Rong Huang
Professor
Chemical Engineering

____

Hung T. Chen
Professor
Chemical Engineering

____

David S. Kristol
Associate Professor
Chemistry

____

James L. Martin
Associate Professor
Mechanical Engineering

____

Angelo J. Perna
Professor
Chemical Engineering

Date Approved: May 6, 1980

ABSTRACT

Title of Thesis: Correlation of Thixotropic Parameters and Related Tests of Blood from Human Subjects

Walter Fabisiak, Doctor of Engineering Science, 1980

Thesis directed by: Ching-Rong Huang
Professor
Chemical Engineering

The flow behavior of human blood is an important facet of the circulatory system as it affects all of the organs of the body. The rheological properties of whole blood provide a means of analyzing the flow of red cells and plasma through the microcirculation. A recently observed rheological characteristic of whole human blood is thixotropy, a time-dependent phenomenon. This phenomenon is caused mainly by the redistribution of an aggregated form of erythrocytes, known as rouleaux, and the non-aggregated, single erythrocytes. In order to further define and analyze the thixotropic properties of blood, the Huang model is used to quantitatively characterize the rheological behavior and relate recorded alterations in blood viscosity at low shear rates to the biophysical parameters of blood elements. Analysis of the various parameters defined by the rheological equation is used to characterize the flow properties of whole blood and provide quantitative comparison among blood samples under a variety of clinical conditions.

Rheological determinations and standard clinical hematological evaluations were performed on sixteen normal sub-

jects and compared with similar data obtained from patients suffering from either polycythemia, Parkinson's disease, or hypertension. In addition, the data of thirteen normal males was compared to that of a group of apparently healthy males who exhibited high levels of one or more of the following coronary risk factors: cigarette smoking, serum cholesterol and diastolic blood pressure. Data analysis for the sample groups was performed for the mean and variance of the group value. Analysis of variance was performed using the standard F-test, and the Student t-test for small sample sizes was used to test for significance in the difference of means.

An analytical solution of the Navier-Stokes equation is presented for the case of a transient flow curve using a Couette geometry. Analysis of the solution indicates that it is possible for a Newtonian fluid to exhibit a hysteresis loop effect in its flow curve under certain experimental conditions. The size and shape of the generated loop was found to be controlled by a dimensionless group. This analysis can be used to detect and eliminate the presence of any artificial hysteresis loop effects such that the true non-Newtonian behavior of a material may be examined.

VITA

Name: Walter Fabisiak

Degree and date to be conferred: D. Eng. Sc., 1980

Secondary education: Harrison High School, 1967

Collegiate Institutions Attended	Dates	Degree	Date of Degree
Newark College of Engineering	1967-1971	BS.Ch.E.	June, 1971
Newark College of Engineering	1971-1974	MS.Ch.E.	October, 1974
New Jersey Institute of Technology	1974-1980	D.Eng.Sc.	May, 1980

Major: Chemical Engineering

Publications:

"Separation of Multicomponent Mixtures via Thermal Parametric Pumping", H.T. Chen, W.W. Lin, J.D. Stokes, W. Fabisiak, A.I.Ch.E. JOURNAL, 20, 306, (1974).

"Quantitative Characterization of Thixotropy of Whole Human Blood", C.R. Huang, N.S. Siskovic, R.W. Robertson, W. Fabisiak, E.H. Smitherberg, A.L. Copley, Biorheology, 12, 279, (1975).

"Thixotropic Parameters of Whole Human Blood", C.R. Huang, W. Fabisiak, Thrombosis Research, 8, Suppl, II, 1, (1976).

"Correlation of Thixotropic Parameters with Application Properties of Latex Paints", C.R. Huang, N.L. Polston, W. Fabisiak, Proceedings of the VII International Congress on Rheology, (1976).

"Mathematical Analysis of the Hysteresis Rheogram of Human Blood", W. Fabisiak and C.R. Huang, Paper 12-5. Presented at the Third International Congress on Biorheology, San Diego, 1978.

"Altered Rheological Properties of Blood During Cardio-pulmonary Bypass", C.R. Huang, J.S. Su, W. Fabisiak, C. Anadhi, P.E. Engler, B. Geissler, J.D. Cohn and S.F. Redo, Paper 17.1, Presented at the 31st Annual Conference on Engineering in Medicine and Biology, Atlanta, 1978.

"A Rheological Equation Characterizing Both the Time-dependent and Steady-state Viscosity of Whole Human Blood", C.R. Huang and W. Fabisiak, AIChE Symposium Series, 182, Vol. 74, 19-21, (1978).

Positions held:

October, 1979 to present

Research Engineer
Celanese Research Company
Summit, New Jersey 07901

September, 1977 to June, 1979

Instructor in Chemical Engineering
Manhattan College
Riverdale, New York 10471

September, 1976 to August, 1977

Special Lecturer in Chemical Engineering
New Jersey Institute of Technology
Newark, New Jersey 07102

January, 1973 to July, 1976

Adjunct Instructor in Chemical Engineering and Chemistry
New Jersey Institute of Technology
Newark, New Jersey 07102

April, 1970 to July, 1971

Engineering Technician
Computer Specialties Corporation
Hackensack, New Jersey

ACKNOWLEDGEMENTS

The author would like to express his deep appreciation and gratitude to his advisor, Dr. Ching-Rong Huang for his guidance and assistance.

The author would also like to thank Dr. Norman Lasser of St. Michael's Medical Center and Dr. Robert Pocelinko of Beth Israel Medical Center for providing the blood samples used in this investigation.

The author would like to thank his wife, Anna-Margaret, for her assistance in the preparation of the manuscript.

TABLE OF CONTENTS

Chapter		Page

LIST OF FIGURES

LIST OF TABLES

CHAPTER I

INTRODUCTION

The rheological behavior of blood is a basic physical property which is essential to the study of intravascular flow. It has physiological significance because it controls the circulation of blood which, in turn, affects all organs. The rheological behavior of blood can be related to the volumetric flow rate of blood, the cardiac energy output, the blood pressure, the distribution of aggregated and non-aggregated forms of erythrocytes, the velocity profile in vivo, the shear stresses of the blood and blood vessels and the rate of shear of the blood. For these reasons, any hindrance to the flow of blood due to an alteration of its rheological behavior is bound to have a direct bearing on the performance of the circulatory system.

Rheology

Rheology is considered to be the science that deals with the deformation and flow of a material. Of all the fluid properties, the viscosity requires the greatest consideration in the study of rheology. Viscosity is considered to be that property of a fluid by virtue of which the fluid offers resistance to deformation or shear. The concept of viscosity is a simple one, but it is not always easy to quantify. Simple fluids exhibit rheological behavior that follows Newton's law of viscosity and for these fluids, the viscosity is an easily determined quantity. Blood is a suspension system consisting of aggregated and non-aggregated forms of erythrocytes suspended in plasma as the continuous phase. Because of the complex nature of blood from a rheological viewpoint, the simple question "What is the normal blood viscosity for a healthy human subject?" has no simple answer. The resistance of blood to deformation or shear is not a constant, but is a shear rate-dependent and time-dependent quantity.

Hemorheology

Blood was observed as a time-dependent, non-Newtonian fluid by Copley (1) in 1941. Copley (2) also introduced the term hemorheology in 1952 to describe the selective rheological investigation of blood. The use of hemorheology in the detection and prevention of diseases is a rapidly developing area of research. Researchers investigating the rheology of humans soon learn that there is usually a significant difference between the rheological behavior of blood from healthy subjects and that from patients with certain pathological disorders. In 1962, Dintenfass (3) observed that, under certain experimental conditions, the blood viscosity of patients who had suffered from myocardial infarction or arterial thrombosis was four to ten times higher than the blood viscosity of healthy subjects. Dintenfass has become a pioneer in the area of hemorheology research and introduced the concepts of viscosity factors, hyperviscosity and viscosity receptors. His investigations in hemorheology are summarized in his books (4,5). In 1971, Aronson et al (6), studied the effect of oral contraceptives on the blood viscosity of healthy young women. They reported the development of clinical signs of thrombophlebitis in one patient who had exhibited the highest and sharpest rise in blood viscosity. In 1974, Stormer et al (7) investigated the blood viscosity of patients suffering from peripheral vascular diseases. They discovered that, under certain experimental conditions, the blood viscosity among the patients was significantly higher than the blood viscosity of healthy subjects. Also in 1974, Chmiel (8) demonstrated the use of hemorheology as a diagnostic tool for predicting myocardial re-infarction.

Quantitative Hemorheology

Although the rheology of blood has been under investigation for many years, investigators have only recently attempted to describe the rheological behavior in terms of quantities other than just the concept of viscosity. In 1963, Cokelete et al (9) applied the two-parameter suspension model proposed by Casson (10) to the study of blood. Their work represented an improvement over the attempts to characterize the rheological behavior by using Newton's law of viscosity. Many variations and modifications of the Casson equation have been attempted with varying degrees of success. Although the literature is strewn with Casson-type equations for describing the rheological behavior of blood, they are all inadequate when it comes to describing the time-dependent behavior of blood. Although Casson's development is based upon the formation of a suspension structure that is rodlike in nature, his final equations may only be applied to steady shearing flows.

In 1942, Copley et al (11) demonstrated the existence of thixotropy in human blood. Thixotropy is a time-dependent phenomenon associated with material systems in which the viscosity depends upon the time and the rate of shear. Thixotropic system behavior is reversible with the thixotropic recovery time depending upon the conditions of the test and on the intrinsic properties of the fluid being tested. Dintenfass (12) examined the thixotropic behavior of blood at very low shear rates. In 1972, Huang et al (13) demonstrated that blood exhibited a classical thixotropic phenomenon, namely, that its flow curve of shear stress versus shear rate was a hysteresis loop. In 1973, Huang et al (14) proposed that the thixotropic behavior of blood is caused by the progressive disaggregation of aggregated erythrocytes, a mechanism for which they presented experimental evidence. In 1975, Huang et al (15) presented a quantitative characterization of the thixotropy of whole human blood in terms of a five parameter rheological equation. Huang and Fabisiak (16) subsequently used this model to examine the thixotropic parameters of blood from different adult males in an attempt to quantify rheological differences in the samples.

At the present time, the most widely used method for studying the rheological behavior of blood is to obtain blood viscosity at different shear rates in steady shear flow. There are disadvantages to using a set of values of blood viscosity at different shear rates to characterize the rheological behavior of blood. Even a number of values of the viscosity of blood at different shear rates is insufficient to completely characterize the rheological behavior of blood because the time-dependent behavior of blood has been omitted. Also, the values of viscosity at low shear rates do not retain their physical meaning because they have been determined from Newton's law of viscosity. This is significant when the shear rates are in the vicinity of that at which blood exhibits a yield stress. In order to give a complete representation of the rheological behavior of blood, a generalized rheological equation is needed to describe the viscosity behavior of blood. This equation can be used to quantitatively represent the rheological behavior of blood and can be used to calculate the blood viscosity at a given shear rate and a given time of shearing. The representation of the rheological behavior of blood by means of a generalized rheological equation is superior to the representation that is given by viscosity values at different shear rates. By knowing the appropriate values of the different parameters in the rheological equation, one can calculate the viscosity of blood at any shear rate and at any time of shearing. Also, the use of rheological parameters should eliminate any uncertainties in the viscosity determined at very low shear rates. This type of rheological description should offer a more accurate picture of the flow behavior of blood.

CHAPTER II

BLOOD AND THE CIRCULATORY SYSTEM

The human circulatory system has as its primary function the delivery of metabolites to the disperse reaction sites of the body and to remove waste products. Other functions of the circulatory system include: the removal of excess heat generated by catabolic chemical reactions in order to maintain the isothermal state of the body, the adjustment of the water and salt levels of the body, the distribution of hormones, natural antitoxins, and drugs from their sites of manufacture or entrance to their sites of action, and self-maintenance operations such as sealing leaks, pH adjustment, and the replacement of components.

The most important feature of the circulatory system is that it is a continuous circuit. If a given amount of blood is pumped by the heart, this same amount must flow through each respective subdivision of the circulatory system. There are two major subdivisions of the circulatory system: the systemic circulation and the pulmonary circulation. The vessels of the circulatory system offer differing amounts of resistance to flow with the larger vessels offering less resistance than the smaller vessels. To overcome this flow resistance, the heart pumps blood into the arteries under pressure, normally at a systolic pressure of 120 mmHg in the systemic circulation and 22 mmHg in the pulmonary system (17). The study of the physical characteristics of blood and the physical principles of blood flow through vessels is called hemodynamics.

Blood

The highly colored, complex fluid of the circulatory system is blood. Under normal conditions, there is no blood outside the circulatory system. Transfer functions between the blood and the various organs of the body must occur across the walls of the circulatory system. There are about five to six liters of blood in the average human being. The blood is pumped by a four-chambered, positive displacement pump called the heart at a rate of about 5 liters per minute, so that the circulation time throughout the body is of the order of one minute.

Blood itself is an aqueous suspension of a straw-colored liquid medium called plasma and several kinds of cells. These include the red blood cells (erythrocytes), the white blood cells (leukocytes), and the platelets (thrombocytes). More than 99% of the cells are red blood cells and, for the most practical purposes, the red blood cells play the major role in determining the physical characteristics of the blood (17). The hematocrit of blood is the percentage of blood that is cells. A numerical value for the hematocrit indicates the percentage of the blood volume that is composed of red cells only. The normal values for the hematocrit are 42 for males and 38 for females, and these values may vary significantly (17).

Plasma

Plasma is a buffered salt solution containing proteins and other macromolecules in a total amount of about 7.5 g/100ml. For many physiochemical purposes, plasma may be treated simply as a 0.155M electrolyte solution buffered to a pH of approximately 7.4. Plasma contains simple proteins, lipoproteins, mucoproteins, and glycoproteins. The major types of proteins found in the plasma are albumin, the globulins, and fibrinogen. The primary function of albumin is to create osmotic pressure at the capillary membrane. This colloid osmotic pressure prevents the plasma fluid from leaking out of the capillaries. The globulins are divided into three major groups: alpha, beta, and gamma globulins. The alpha and beta globulins perform diverse functions in the circulatory system, while the gamma globulins play a special role in the body's immune system. Fibrinogen is a high molecular weight protein found in the plasma in quantities of 100 to 700 mg/100ml. Fibrinogen is of basic importance in the blood clotting process. It is converted into fibrin by the enzyme thrombin and the fibrin polymerizes into fibrin threads that enmesh red blood cells and plasma to form a blood clot. Fibrinogen is a vital constituent of one of the major steps in blood coagulation.

Blood Cells

The red blood cells are normally present in very high numbers of the order of five million per cubic millimeter. The mature red blood cell is a flexible, biconcave disc of a diameter of about 8.5 microns and a thickness that varies from 1.0 to 2.4 microns. In normal blood flow, the cells are suspended individually, but at very low flow rates and in abnormal situations, they aggregate into stacks of cells called rouleaux. Since the rouleaux behave as single units, their formation can bring about marked changes in the hemodynamic behavior of blood. The white blood cells are present in the order of five to eight thousand per cubic millimeter, which represents only about 0.15% of the red cell number. This represents an insignificant volume fraction of the blood and so the importance of the white cells is not in hemodynamics. The normal platelet count is about 10% of the red cell count. They are distributed unevenly in the circulation with a greater number being in the pulmonary blood. The platelets are oval, flat, non-nucleated cells of two to four microns in diameter. They are important in blood clotting as they tend to adhere to damaged areas in the vascular wall.

Various diseases of the circulation that cause decreased blood flow through the peripheral vessels increase the rate of red cell production. This is especially apparent in prolonged cardiac failure and many lung diseases for the tissue hypoxia resulting from these conditions increases the red cell production with resultant increases in hematocrit and total blood volume. Any condition that causes the quantity of oxygen transported to the tissues to decrease, ordinarily increases the rate of red cell production. The functional ability of the red blood cells to transport oxygen to the tissues in response to the tissue demand for oxygen is the controlling factor in red cell production. Anemia refers to a deficiency of red blood cells. Since the viscosity of blood is a function of the concentration of red blood cells, anemia can drastically reduce the blood viscosity (17). Decreased blood viscosity decreases the resistance to blood flow in the peripheral vessels so that greater than normal quantities of blood are returned to the heart. As a consequence, the cardiac output increases. Hypoxia causes the tissues to dilate and increases the return of blood to the heart and also increases the cardiac output. One of the major effects of anemia is an increase in the work-load of the heart. The increased cardiac output in anemia offsets many of the symptoms of anemia. The rate of blood flow is increased to such an extent that almost normal quantities of oxygen are delivered to the tissues.

Whenever the tissues become hypoxic because of too little oxygen in the atmosphere or because of failure of delivery of oxygen to the tissues, the blood forming organs automatically produce large quantities of red blood cells. This condition is called secondary polycythemia and the red cell count commonly rises to as high as six to eight million per cubic millimeter. In addition to those people having secondary polycythemia, others may have a condition known as polycythemia vera in which the red cell count may be as high as nine million per cubic millimeter and the hematocrit as high as 70 to 80%. Polycythemia vera is a tumorous condition of the blood cell producing organs. It causes an excess production of red blood cells in the same manner that a muscle tumor causes excess production of a specific type of muscle cell. Polycythemia vera also increases the total blood volume and, as a result, the entire vascular system becomes intensely engorged with many of the capillaries being plugged by the very viscous blood. With this increased viscosity, blood flow through the vessels is extremely sluggish. The increase in total blood volume also increases the circulation time through the body. The mean circulation time may be as high as twice that of the normal value. Thus, the velocity of blood flow in any given vessel is considerably decreased in polycythemia.

Circulatory System

Four factors complicate the fluid mechanical analysis of the circulatory system: the complexity of the fluid, the periodic nature of the flow, the elasticity of the system boundaries, and the high level of integration of the system. The intrinsic flow properties of blood are not simple because the structure of blood is both complex and unstable. The viscoelastic behavior of the red cell's contents are not well understood nor are the forces which hold the cell in its normal biconcave configuration. The cell membrane is viscoelastic and the cells are capable of aggregating as rouleaux or clumps and may change their shape. The plasma phase is essentially Newtonian, but contains fibrinogen which mediates aggregative processes. The measurement of suspension properties is complicated by the tendency of the cells and the suspending fluid to separate because of both static and dynamic forces.

Since most of the resistance to flow in the circulatory system occurs in the small blood vessels, it is important to know how the blood viscosity affects blood flow in these minute vessels. Flow through a blood vessel is determined entirely by two factors: the pressure differential tending to push blood through the vessel, and the vascular resistance through the vessel. This may be expressed mathematically as

$$Q = \Delta P/R_V \qquad (2\text{-}1)$$

where Q is the volumetric rate of blood flow, ΔP is the pressure difference between the two ends of the vessel and R_V is the vascular resistance. The overall blood flow in the circulation of an adult person at rest is about five liters per minute. This is referred to as the cardiac output and passes through both the systemic and pulmonary circulations.

When blood flows at a steady rate through a long, smooth vessel, it flows in streamlines and concentric layers within the vessel. This is known as laminar flow. When the blood is flowing in all directions within the vessel and continually mixing within the vessel, turbulent flow occurs. In laminar flow, the velocity profile within the vessel takes on a parabolic shape with the maximum velocity occurring at the center of the vessel. During turbulent flow, the blood will flow crosswise in the vessel as well as along the vessel, usually forming swirls called eddy currents. These eddy currents offer a much greater resistance to blood flow. The occurrence of either type of flow is normally determined by the evaluation of the Reynolds number, defined as

$$N_{Re} = \frac{\rho v d}{\mu} \tag{2-2}$$

where ρ is the fluid density, v is the average fluid velocity, d is the vessel diameter, and μ is the fluid viscosity. Turbulent flow occurs at vessel branches at Reynolds numbers in excess of 200 and occurs in straight vessels for Reynolds in excess of 2000.

Resistance is the impediment to blood flow in a vessel. It cannot be measured by direct means, but must be estimated from measurements of blood flow and pressure differences in the blood vessel. If the pressure difference between two points in a vessel is one mm Hg and the flow is one ml/s, then the resistance to flow is said to be one peripheral resistance unit:

$$PRU = \frac{1 \text{ mm Hg}}{1 \text{ ml/s}} \tag{2-3}$$

The resistance of the entire systemic circulation is approximately one PRU. In some conditions in which the blood vessels become constricted, the total peripheral resistance may rise as high as four PRU, and when the vessels become greatly dilated, the resistance may drop to 0.25 PRU. The total pulmonary resistance at rest is about 0.09 PRU, and can rise as high as 1.0 PRU or drop to as low as 0.03 PRU.

Conductance is a measure of the amount of blood that can pass through a vessel in a given amount of time for a given pressure difference. It is merely the reciprocal of resistance. A generalized relationship for laminar flow in circular tubes is the Hagen-Poiseuille equation

$$Q = \frac{\pi \Delta p r^4}{8 \mu L} \qquad (2\text{-}4)$$

where Q is the volumetric flow rate, Δp is the pressure difference, r is the vessel radius, L is the vessel length, and μ is the blood viscosity. The quantity of blood that will flow through a vessel in a given period of time is equal to the product of the vessel cross-sectional area and the average velocity

$$Q = v \pi r^2 \qquad (2\text{-}5)$$

Using the Hagen-Poiseuille equation, we can develop expressions for the vascular conductance and resistance

$$C_V = \frac{\pi r^4}{8 \mu L} \qquad (2\text{-}6)$$

$$R_V = \frac{8\mu L}{\pi r^4} \tag{2-7}$$

Note that the viscosity plays an important role in the determination of either conductance or resistance and is the only physical blood parameter which is a factor in the flow of blood. It is for this reason that the study of the viscosity of blood is an important research area that needs further investigation.

CHAPTER III

CLASSIFICATION OF FLUID BEHAVIOR

Fluids are normally subdivided into Newtonian and non-Newtonian categories based upon their flow behavior. These characterizations are normally based upon the shear stress response of the fluid to some applied shear field. These responses are usually presented graphically in the form of rheograms. There are many types of rheograms, but the two most widely reported are the plot of shear stress versus shear rate and the plot of shear stress versus time at a constant shear rate. The former is often referred to as the flow curve of the fluid and the latter is known as the torque-decay curve of the fluid. The flow behavior is often represented by means of a rheological equation. This equation would describe the functional relationship between the shear stress response and the applied shear field. A generalized rheological equation may be simply expressed as

$$\tau = f(\dot{\gamma}) \qquad (3\text{-}1)$$

where τ is the shear stress and $\dot{\gamma}$ is the shear rate.

Newtonian Fluids

The simplest type of rheological behavior is exhibited by what are referred to as Newtonian fluids. Newtonian fluids exhibit a direct proportionality relationship between the shear stress response and the applied shear rate. The proportionality constant is called the Newtonian viscosity.

The flow curve for a Newtonian fluid is a straight line passing through the origin having a slope that is equal to the Newtonian viscosity. The torque-decay curve of a Newtonian fluid is flat, indicating that the fluid exhibits no time-dependent behavior. Typical Newtonian fluid rheograms are shown in Figure 1. Newtonian fluid behavior is usually represented by the following rheological equation

$$\tau = -\mu\dot{\gamma} \qquad (3\text{-}2)$$

where μ represents the Newtonian viscosity. This equation is often called Newton's law of viscosity. The minus sign is used to adhere to conventional notation as used in classical texts such as Bird et al. (18). Fluids that do not exhibit this simple behavior are referred to as being non-Newtonian.

Non-Newtonian Fluids

Non-Newtonian fluids are those fluids for which the shear stress response is not a linear function of the applied shear rate. Non-Newtonian behavior is most pronounced at intermediate rates of shear. At very high or very low shear rates, many non-Newtonian fluids exhibit Newtonian-like behavior. Therefore, a material may only be classified as being non-Newtonian for a specified range of shear rates. Furthermore, these fluids can be subdivided into time-dependent and time-independent categories. Time-independent non-Newtonian fluids are those for which the shear stress

FIGURE 1: NEWTONIAN FLUID RHEOGRAMS

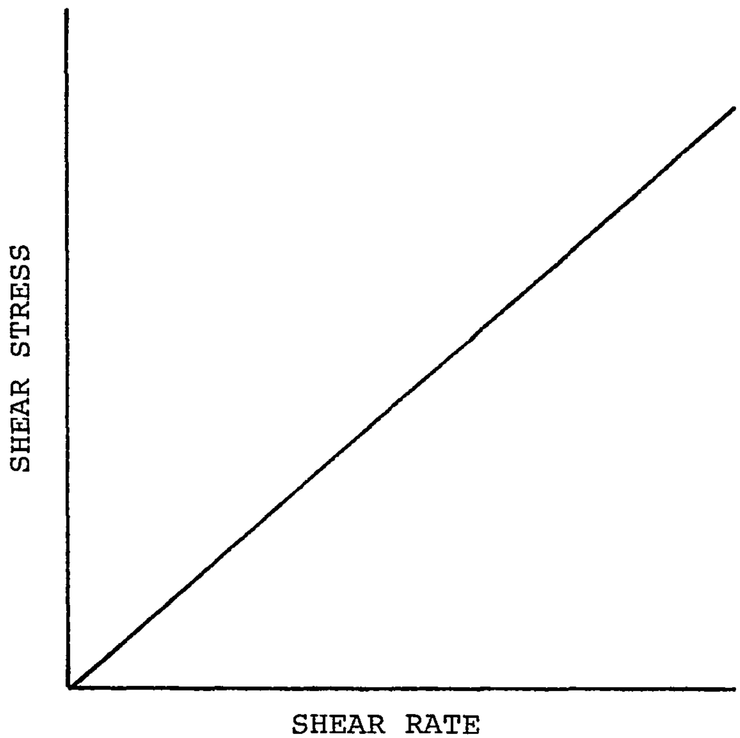

Flow Curve

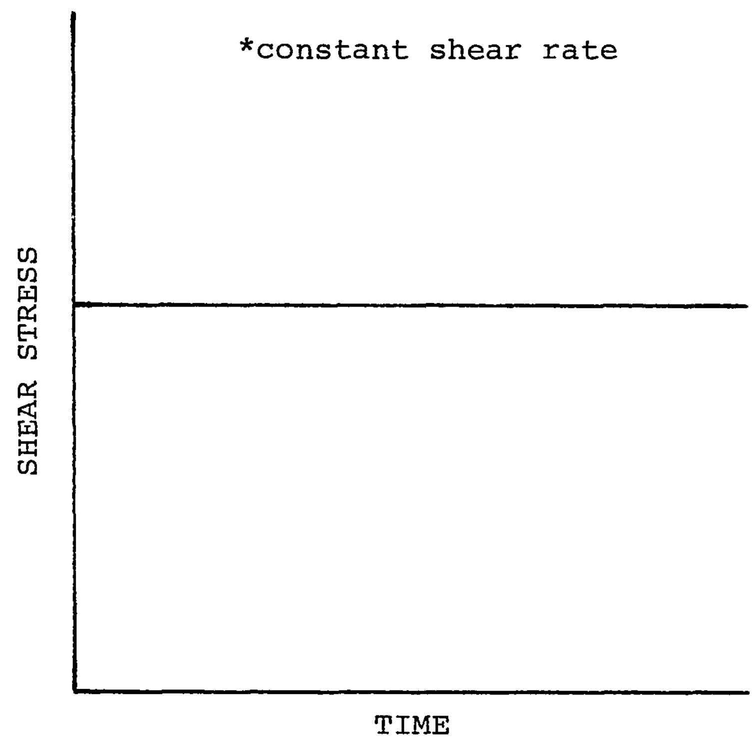

Torque-Decay Curve

response is only a function of the shear rate. A classical example of a time-independent, non-Newtonian fluid is a pseudoplastic material. It possesses a nonlinear flow curve which may or may not pass through the origin, although its torque-decay curve is similar to that of a Newtonian fluid. If the flow curve does not pass through the origin, the fluid is said to possess a yield stress, τ_0. The fluid will not flow until the shear stress response exceeds that of the yield stress. A finite shear rate may be applied to such a material without the fluid actually beginning to flow. Many fine suspensions and pastes exhibit a yield stress. Typical pseudoplastic fluid rheograms are shown in Figure 2. Pseudoplastic behavior is usually represented in equational form using an empirical power law relationship

$$\tau = -k\dot{\gamma}^{m} \tag{3-3}$$

where k is called the consistency index and m is called the flow behavior index of the fluid. The numerical value of the flow behavior index is always less than one for pseudoplastic fluids. The power law is the simplest rheological equation used to describe pseudoplastic behavior, although there have been many attempts to develop equations capable of representing pseudoplastic behavior. Skelland (19) has summarized many of the more popular pseudoplastic equations. Casson (10) has developed a rheological equation, capable of representing pseudoplastic behavior, that has found wide

FIGURE 2: PSEUDOPLASTIC FLUID RHEOGRAMS

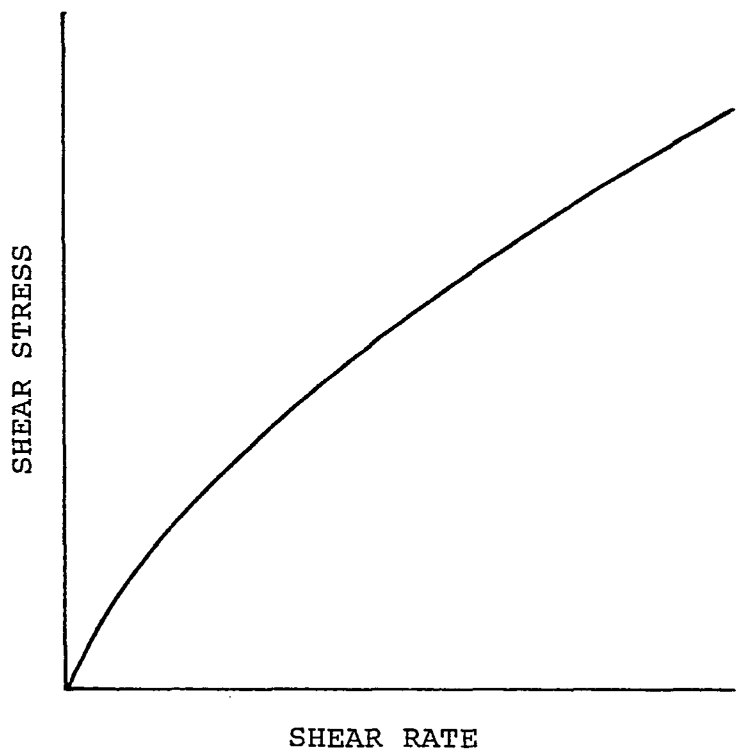

Flow Curve

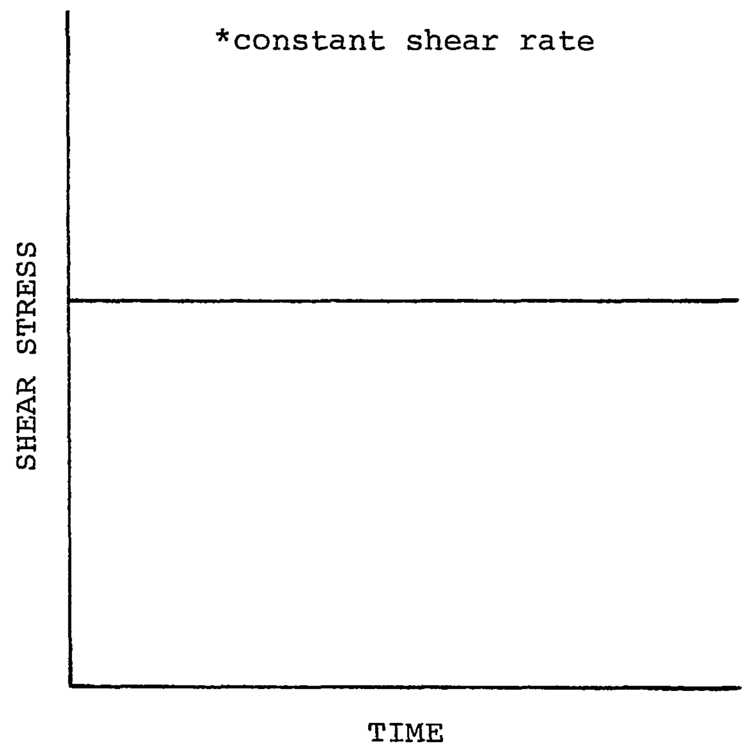

Torque-Decay Curve

acceptance in the correlation of the rheological behavior of time-independent, non-Newtonian materials. The Casson model was originally developed to describe the behavior of printing inks and is expressed as

$$\sqrt{\tau} = k_0 + k_1\sqrt{\dot{\gamma}} \qquad (3-4)$$

where k_0 and k_1 are functions of phases of the fluid under observation and are constant for a given fluid. Casson's model is quite popular because it is not empirical in nature, but has a theoretical foundation since it was developed as a suspension model in which mutually attractive particles are suspended in a Newtonian medium. These particles are capable of aggregating at low shear rates to form rodlike structures.

By analogy to the definition of the Newtonian viscosity, an apparent viscosity for non-Newtonian fluids may be defined as follows

$$\eta = -(\tau/\dot{\gamma}) = f(\dot{\gamma}) \qquad (3-5)$$

where η is called the apparent viscosity. A value for the apparent viscosity is without meaning unless it is accompanied by the corresponding shear rate. Again, the minus sign is used by convention. Therefore, the apparent viscosity for a power law fluid is

$$\eta = k(\dot{\gamma})^{m-1} \qquad (3-6)$$

It must be emphasized that the apparent viscosity is only analogous to the Newtonian viscosity and no direct comparison can be made without the stipulation of the shear rate.

For time-dependent, non-Newtonian fluids, the shear stress response is not only a function of the shear rate, but is also a function of the shear history. Thixotropic fluids are classic examples of time-dependent, non-Newtonian fluids. The apparent viscosity of a thixotropic fluid is a function of the rate of shear and of the duration of shear. This may be expressed in general terms as

$$\eta = f(\dot{\gamma}, t) \qquad (3\text{-}7)$$

where t is time. The rheological behavior of thixotropic fluids has the following characteristics: (a) an isothermal structural change is brought about by applying a mechanical disturbance to the system, (b) when the mechanical disturbance is removed, the system recovers its original structure only after a certain elapsed time, depending upon the material, and (c) the flow curve of the system exhibits an hysteresis effect. The hysteresis loop behavior of the shear stress response is obtained by subjecting the system to a linear increase in the shear rate up to some maximum value and then immediately decreasing the shear rate to the initial value at the same rate. Thus, the flow curve of a thixotropic material consists of a distinct upcurve and a distinct downcurve, whereas the upcurve and the downcurve for Newtonian and time-independent, non-Newtonian fluids are coincident. The torque-decay curve for a thixotropic fluid also differs from that of a Newtonian or a time-independent, non-Newtonian fluid. Typical thixotropic fluid rheograms are shown in Figure 3. A thixotropic material may exhibit time-independent, non-Newtonian behavior after an extended period of shear, but will regain its thixotropic behavior once the shear field is removed and the material is permitted to regain its internal structure. Under extremely high rates of shear for extended periods, a thixotropic fluid may even exhibit Newtonian behavior, but will also regain its thixotropic behavior upon removal of the shear field, as long as there has been no irreversible damage induced upon the suspended phase. This complex behavior has led to extreme difficulty in the attempts to obtain a satisfactory rheological model that will represent the various thixotropic phenomena. Rheological equations such as the power law and Casson model are not sufficiently versatile to completely characterize thixotropic behavior. These models are incapable of representing the time-dependent behavior of thixotropic materials. Orosz (20) has presented a synopsis of thixotropic equations which are capable of representing some of the various thixotropic phenomena. He indicates that most of the equations available in the literature are unable to express all of the various thixotropic phenomena. Some equations are specific and can describe a particular property associated with thixotropy, but most are

FIGURE 3: THIXOTROPIC FLUID RHEOGRAMS

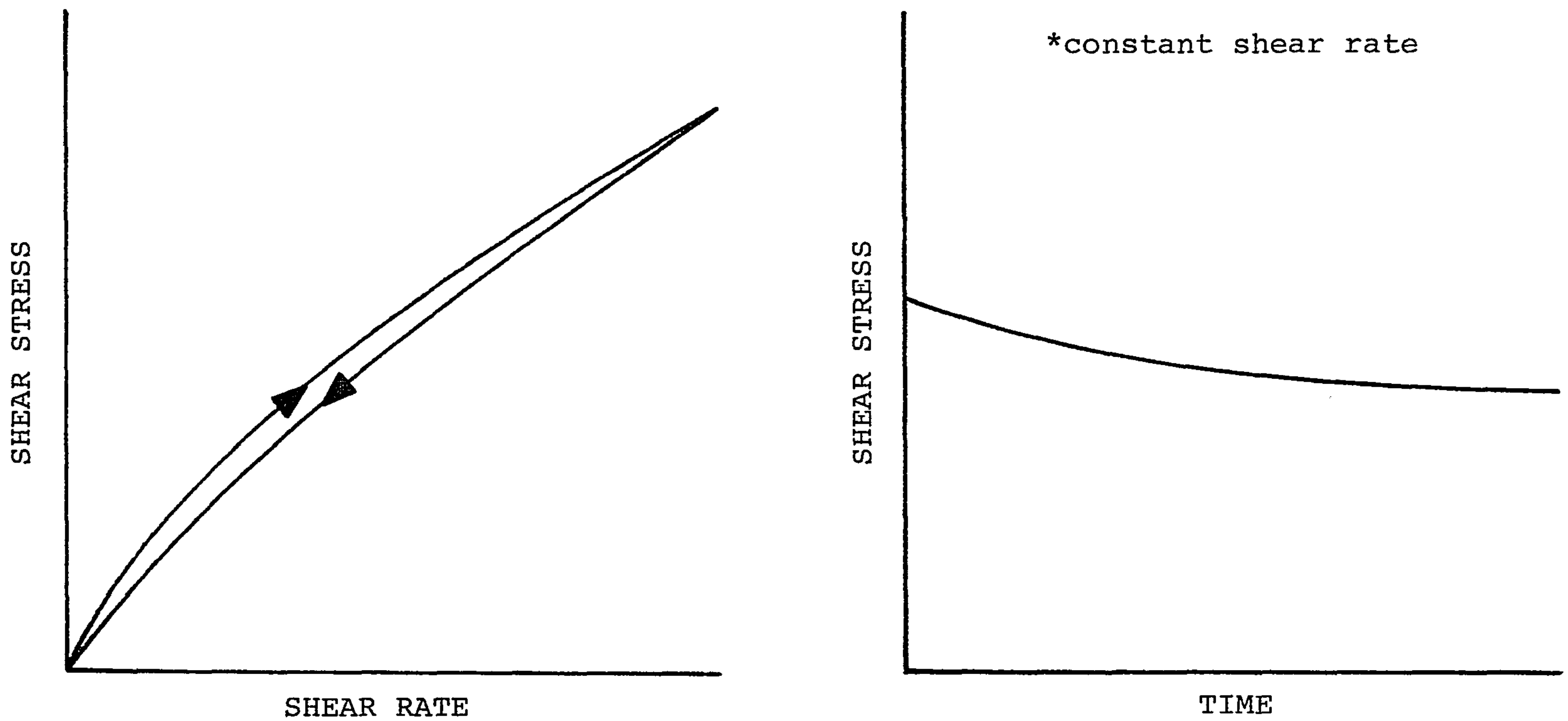

Flow Curve

Torque-Decay Curve

not general enough to be used to completely characterize a thixotropic material.

Huang Model

Recently, Huang (21) has developed a generalized rheological model that is capable of representing the thixotropic behavior of a fluid. The model is based upon irreversible thermodynamics and assumes that there exists a progressive structural breakdown of a molecular arrangement parameter. This structrual breakdown is effected by a mechanical disturbance induced by a shear field. For thixotropic materials, the Huang model takes the following form

$$\tau = \tau_0 + \mu\dot{\gamma} + c_1 A\dot{\gamma}^n \exp[-c_1 \int_0^t |\dot{\gamma}|^n dt] \qquad (3\text{-}8)$$

where c_1 is a kinetic rate constant of the structural breakdown, A is a constant related to the equilibrium value of the molecular arrangement parameter when the fluid is not under the influence of shear for a long period of time, and n is the order of the structural breakdown reaction. Under the appropriate conditions, the Huang model can be applied to represent both the flow curve and the torque-decay curve rheograms. Using the appropriate mathematical expression for the shear rate in the integral portion of the Huang model will result in algebraic expressions for the upcurve, downcurve, and the torque-decay curve. For the upcurve, a ramp function is used to represent the shear rate

$$\dot{\gamma} = \alpha t \qquad (3\text{-}9)$$

where α is a proportionality constant. Therefore, the Huang equation becomes for $0 \leq t \leq t_1$

$$\tau = \tau_0 + \mu\dot{\gamma} + c_1 A\dot{\gamma}^n \exp[-c_1\dot{\gamma}^{(n+1)}/(\alpha(n+1))] \qquad (3\text{-}10)$$

where t_1 is the time required to bring the shear rate up to its maximum value. For the downcurve, a declining ramp function is used in the integral

$$\dot{\gamma} = 2\alpha t_1 - \alpha t \qquad (3\text{-}11)$$

The Huang equation now becomes for $t_1 \leq t \leq 2t_1$,

$$\tau = \tau_0 + \mu\dot{\gamma} + c_1 A\dot{\gamma}^n \exp[(-c_1/(\alpha(n+1)))(2\dot{\gamma}_m^{n+1} - \dot{\gamma}^{n+1})] \qquad (3\text{-}12)$$

where $\dot{\gamma}_m$ is the maximum value of the shear rate. For the torque-decay curve, a step function input is used for the shear rate

$$\dot{\gamma} = \dot{\gamma}_c = \text{constant} \qquad (3\text{-}13)$$

The Huang equation now becomes

$$\tau = \tau_0 + \mu\dot{\gamma}_c + c_1 A\dot{\gamma}_c^n \exp[-c_1\dot{\gamma}_c^n t] \qquad (3\text{-}14)$$

Therefore, the Huang model is mathematically capable of representing both rheograms of a thixotropic fluid. Huang et al. (14) have demonstrated the ability of the model to describe the hysteresis loop behavior of a thixotropic material. In a later work, Huang et al. (15) used the model to describe both the hysteresis loop and torque-decay rheograms of a thixotropic material resulting in a quantitative characterization of the thixotropic behavior. Huang and Fabisiak (16) subsequently used the model to examine the thixotropic parameters of whole human blood from different adult males and to quantify rheological differences in the samples. Huang et al. (22) demonstrated the versatility of the model by quantitatively characterizing another thixotropic material, latex paint. In a recent work, Huang and Fabisiak (23) showed that the Huang model could also represent another rheogram, the steady-state viscosity variation with respect to shear rate. They developed the following expression for the steady-state viscosity of a thixotropic material

$$\eta_s = \mu + c_1 A \dot{\gamma}^{n-1} \exp[-c_1 \dot{\gamma}^n t_0] \qquad (3\text{-}15)$$

where η_s is the steady-state viscosity and t_0 is a time constant which is indicative of the duration required for the fluid to change its rheological behavior from thixotropic to pseudoplastic.

Presently, the Huang model has been demonstrated as the most versatile rheological model for thixotropic materials and that it is capable of quantitatively characterizing the observed thixotropic behavior. It is because of its versatility that the Huang model can be used for the quantitative characterization of the thixotropic behavior of human blood.

Since the Huang rheological model was not specifically developed for blood, but for a general thixotropic fluid, it must be examined in light of the nature of blood as a fluid system. The Huang model is based upon the progressive structural breakdown of a fluid network by means of a mechanical disturbance. Blood is a suspension system consisting of aggregated and non-aggregated forms of erythrocytes suspended in a plasma phase. The aggregated form of erythrocytes comprises a structural arrangement known as rouleaux. Huang et al. (14) have proposed that the thixotropic behavior of blood is caused by the progressive breakdown of the rouleaux into individual erythrocytes. This hypothesis is consistent with the development of the Huang model. Now c_1 specifically refers to the kinetic rate constant of the structural breakdown reaction of rouleaux into individual erythrocytes and n is the order of this breakdown reaction. The other Huang model parameters retain their general descriptions.

CHAPTER IV

FLUID DYNAMICS

The rheological behavior of a fluid can be characterized, in general, by its flow curve, which is a diagram relating the shear stress response to an applied shear rate. A rheological equation is then used to represent, mathematically, the flow curve of the fluid. Therefore, unless the flow curve of the fluid is available, it would be difficult to postulate its describing rheological equation of state. Rheological characterization requires obtaining the flow curve from experimental data. The required experimental data is most readily obtained from devices known as viscometers.

Viscometers

There are a variety of commercially available viscometers which are capable of generating the data necessary to obtain the shear stress as a function of the rate of shear or the shear rate as a function of the applied shear stress. They include the capillary tube, falling ball, concentric cylinder, and the cone-and-plate viscometers. When studying time-dependent, non-Newtonian rheological behavior, a viscometer of the rotational type is employed. This restricts the viscometer to either the concentric cylinder variety or the cone-and-plate variety. A rotational viscometer is used for studying thixotropic materials because the viscosity is a function of time as well as a function of the shear rate. For the capillary tube or falling ball viscometers, the tube diameter or the ball density have to be varied to introduce a change in the shear rate. This causes a discontinuity in the time function during the course of an experiment. With a rotational viscometer, however, a change in the rotational speed will change the rate of shear applied to the sample without having to change the sample being analyzed. This variation in shear rate can be performed continuously, either through mechanical means or through the use of an automatic control mechanism.

The sample holder geometry is one of the most crucial aspects of the viscometer. Since the time-dependent nature of the analysis of the rheological behavior of thixotropic materials limits the viscometer to a rotational type, a decision must be made as to which sample holder geometry is best suited for the material being studied. Sinusas (24) made a study of the various sample holder geometries and proposed that the optimum design for a sample holder for studying the rheological behavior of blood is a type of concentric cylinder referred to as a double Couette. He included in his study a detailed analysis of the possible end effects associated with this geometric configuration. The proposed sample holder geometry is displayed in Figure 4.

Double Couette Viscometer

The double Couette viscometer consists of a rotating cylinder having a concentric cylindrical slot. Another concentric cylinder is suspended into this slot with the sample occupying the spaces between the cylinders. The inner cyl-

FIGURE 4: DOUBLE COUETTE VISCOMETER

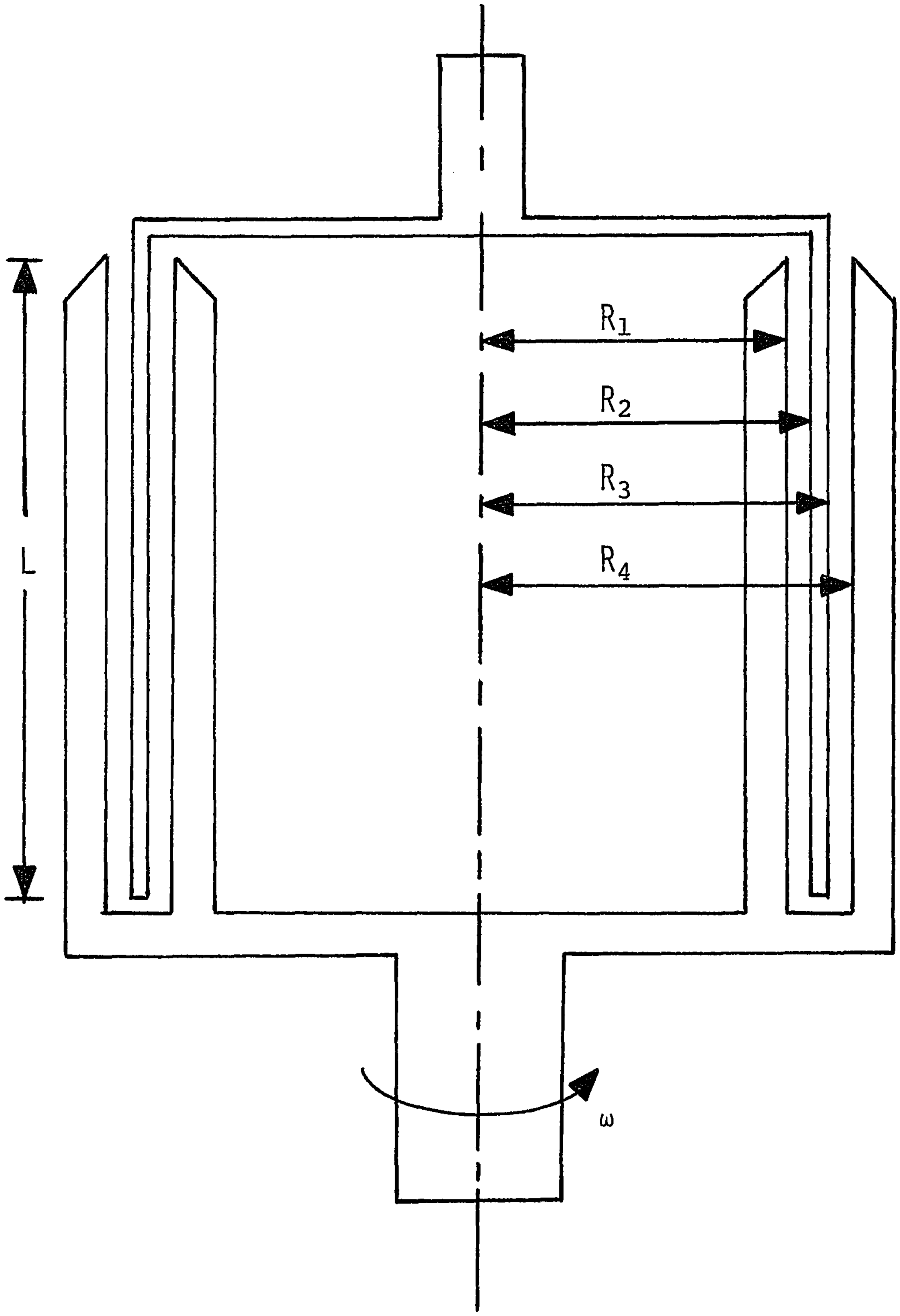

inder does not rotate and is connected to a torque-sensing device. This design is essentially a combination of two Couette viscometers. One portion of the double Couette acts like a concentric cylinder viscometer in which the inner cylinder is stationary with the outer cylinder rotating, while the other portion of the double Couette behaves like a concentric cylinder viscometer in which the inner cylinder is rotating while the outer cylinder is stationary. The length of submersion is L and the four radii of interest are R_1, R_2, R_3, and R_4. The rotational speed of the bottom portion of the double Couette is ω. The usual data obtained from any concentric cylinder are the torque exerted on a stationary fluid-solid boundary and the rotational speed of the moving fluid-solid boundary. The shear stress is related to the torque by solving the equation of motion. Obtaining the shear rate requires the simultaneous solution of the equation of motion and the rheological equation of state. Due to mathematical complexity, an explicit expression for the shear rate has only been solved for a limited number of cases.

For an incompressible, Newtonian fluid undergoing isothermal flow, the equations of continuity and motion are

$$\nabla \cdot \vec{v} = 0 \tag{4-1}$$

$$\rho \frac{\partial \vec{v}}{\partial t} = - \rho [\nabla \cdot \vec{v}\vec{v}] - \nabla p + \mu \nabla^2 \vec{v} + \rho \vec{g} \tag{4-2}$$

where ρ is the fluid density, $\vec{v}$ is the velocity vector, p is the static pressure, μ is the Newtonian viscosity, and $\vec{g}$ is the gravitational force per unit mass. In steady-state laminar flow, the fluid moves in a circular pattern with the velocity in the radial and axial directions assumed to be zero. The angular component of the equation of motion reduces to, under these conditions

$$\frac{d}{dr}\left(\frac{1}{r}\frac{d}{dr}\left(rv_\theta\right)\right) = 0 \qquad (4\text{-}3)$$

Equation (4-3) may be integrated twice to yield the following expression for the angular velocity profile

$$v_\theta = \frac{Cr}{2} + \frac{D}{r} \qquad (4\text{-}4)$$

where C and D are constants of integration to be evaluated from the appropriate boundary conditions. Since there are, in effect, two concentric cylindrical viscometers combined in this situation, there will be two sets of boundary conditions to be satisfied. Equation (4-4) represents the general velocity profile for a fluid flowing between a pair of concentric cylinders and is valid for either portion of the double Couette. Each section of the double Couette will yield a different set of integration constants. For the inner concentric cylinder section, when $R_1 \leq r \leq R_2$, the appropriate boundary conditions are

$$r = R_1;\ v_\theta = 2\pi\omega R_1 \qquad (4\text{-}5a)$$

$$r = R_2;\ v_\theta = 0 \qquad (4\text{-}5b)$$

Applying these boundary conditions to equation (4-4) yields the following expressions for the constants of integration

$$C = \frac{-4\pi\omega R_1^2}{R_2^2 - R_1^2} \qquad (4\text{-}6a)$$

$$D = \frac{2\pi\omega R_1^2 R_2^2}{R_2^2 - R_1^2} \qquad (4\text{-}6b)$$

Incorporating these integration constants into equation (4-4) gives the velocity profile when $R_1 \leq r \leq R_2$,

$$v_\theta = \frac{2\pi\omega R_1^2}{R_2^2 - R_1^2}\left(\frac{R_2^2}{r} - r\right) \qquad (4\text{-}7)$$

For the outer concentric cylinder section, the appropriate boundary conditions are

$$r = R_3;\ v_\theta = 0 \qquad (4\text{-}8a)$$

$$r = R_4;\ v_\theta = 2\pi\omega R_4 \qquad (4\text{-}8b)$$

Using these boundary conditions, the constants of integration become

$$C = \frac{4\pi\omega R_4^2}{R_4^2 - R_3^2} \qquad (4\text{-}9a)$$

$$D = \frac{-2\pi\omega R_4^2 R_3^2}{R_4^2 - R_3^2} \qquad (4\text{-}9b)$$

Incorporating these integration constants into equation (4-4) gives the velocity profile when $R_3 \leq r \leq R_4$,

$$v_\theta = \frac{2\pi\omega R_4^2}{R_4^2 - R_3^2}\left(r - \frac{R_3^2}{r}\right) \qquad (4\text{-}10)$$

Once the velocity profiles have been established, expressions for the evaluation of the shear rate may be obtained. For this particular situation, the $r\theta$ component of the shear rate tensor may be obtained from

$$\dot{\gamma}_{r\theta} = r\,\frac{d}{dr}\left(v_\theta/r\right) \qquad (4\text{-}11)$$

Since we are dealing with a double Couette, there will be two shear rate expressions. When $R_1 \leq r \leq R_2$, the shear rate is

$$\dot{\gamma}_{r\theta}\Big|_{r=R_2} = \left(r\,\frac{d}{dr}\left(v_\theta/r\right)\right)_{r=R_2} = \frac{-4\pi\omega R_1^2}{R_2^2 - R_1^2} \qquad (4\text{-}12a)$$

and when $R_3 \leq r \leq R_4$,

$$\dot{\gamma}_{r\theta}\Big|_{r=R_3} = \left(r\,\frac{d}{dr}\left(v_\theta/r\right)\right)_{r=R_3} = \frac{4\pi\omega R_4^2}{R_4^2 - R_3^2} \qquad (4\text{-}12b)$$

To insure that there is a uniform shear rate on both sides of the immersed cylinder, we impose the following design restriction

$$\dot{\gamma}_{r\theta}\Big|_{r=R_2} = -\dot{\gamma}_{r\theta}\Big|_{r=R_3} \tag{4-13}$$

By equating the two expressions for the shear rate, we obtain the following design constraint

$$\frac{R_1^2}{R_2^2 - R_1^2} = \frac{R_4^2}{R_4^2 - R_3^2} \tag{4-14}$$

The shear stress is related to the shear rate by the generalized rheological equation

$$\tau_{r\theta} = -\eta\dot{\gamma}_{r\theta} \tag{4-15}$$

Due to the design restriction, the following shear stress relationship is valid

$$\tau_{r\theta}\Big|_{r=R_2} = -\tau_{r\theta}\Big|_{r=R_3} \tag{4-16}$$

which merely indicates that the shear stresses exerted on either side of the immersed cylinder are the same. Unfortunately, the shear stresses are not measured quantities, but are related to the total torque exerted on the immersed cylinder. The torque exerted on the inner surface is

$$T_i = 2\pi R_2^2 L\left(\tau_{r\theta}\right)_{r=R_2} \tag{4-17}$$

and the torque exerted on the outer surface is

$$T_o = 2\pi R_3^2 L \left(-\tau_{r\theta}\right)_{r=R_3} \qquad (4\text{-}18)$$

The total measured torque is the sum of these two torque terms

$$T = T_i + T_o = 2\pi L[R_2^2 + R_3^2] \left(\tau_{r\theta}\right)_{r=R_2} \qquad (4\text{-}19)$$

which has been simplified by the relationship given in equation (4-16). Thus, we now have an expression for the shear stress in terms of a measured quantity, namely, the total torque. Therefore, given the dimensions of the double Couette, the rotational speed of the bottom portion, and the measured torque, the corresponding shear rates and shear stresses may be determined.

Transient Flow

These expressions are valid for steady-state flow conditions, but both the torque-decay and flow curve behavior for a thixotropic material are time-dependent. The transient flow of a fluid in a Couette viscometer arrangement was first studied by Bird and Curtiss (25). They have presented an exact solution to the equations of change for the transient, laminar, tangential flow of an isothermal, incompressible, viscous fluid in the annular space between two cylinders, one or both of which may be rotating. Their solution details the mathematics of the torque-decay curve and their velocity profile solution consists of a steady-state portion and a transient portion. The input for the angular rotation of the cylinder is a step function. From their analysis, one can determine the transient hydrodynamic effects for a particular sample in a specified sample holder. By properly selecting the experimental conditions, one can virtually eliminate any undesired transient effects so that the torque-decay behavior being observed is due to the rheological properties of the material only. Their analysis provides a means for eliminating any artificial torque-decay responses. For a material having the approximate kinematic viscosity of human blood, they demonstrate that the anticipated transient response should be small, such that the observed torque-decay curve is truly representative of the rheological behavior of blood.

One of the most important rheological characteristics of human blood is that its flow curve exhibits an hysteresis effect. This hysteresis loop is observed on a plot of the shear stress versus the shear rate in which the shear rate is steadily and linearly increased to a maximum value and then immediately decreased at the same rate to the initial value. Recent investigations (14,15,16,26,27) into the thixotropic behavior of human blood have incorporated hysteresis loop analysis in the quantitative characterization of the rheological behavior. Until recently, no one has examined the mathematical aspects of the hysteresis loop rheogram in a manner analogous to the analysis of the torque-decay rheogram by Bird and Curtiss. Fabisiak and Huang (28) have obtained an analytical solution of the

Navier-Stokes equation for the case of an hysteresis loop rheogram using a Couette geometry. They have analyzed the transient flow under the conditions of a ramp function angular velocity. The ramp function angular velocity input is required to generate the flow curve. This ramp function input is shown in Figure 5. They have examined a general Couette viscometer in which the fluid occupies the annular region between a pair of concentric cylinders having radii of κR and R, with a length L(see Figure 6). At time $t < 0$, the fluid within the annulus is at rest. At time $t > 0$, the inner cylinder remains stationary and the outer cylinder is subjected to a ramp function change in its angular velocity. For an incompressible, Newtonian fluid in this application, the equation of motion reduces to

$$\rho \frac{\partial v_\theta}{\partial t} = \mu\frac{\partial}{\partial r}\left(\frac{1}{r}\frac{\partial}{\partial r}\left(r v_\theta\right)\right) \tag{4-20}$$

The appropriate initial and boundary conditions are

$$v_\theta(r,0) = 0 \tag{4-21a}$$

$$v_\theta(\kappa R,t) = 0 \tag{4-21b}$$

$$v_\theta(R,t) = F(t) \tag{4-21c}$$

where the ramp function $F(t)$ is defined as

FIGURE 5: RAMP FUNCTION ANGULAR VELOCITY

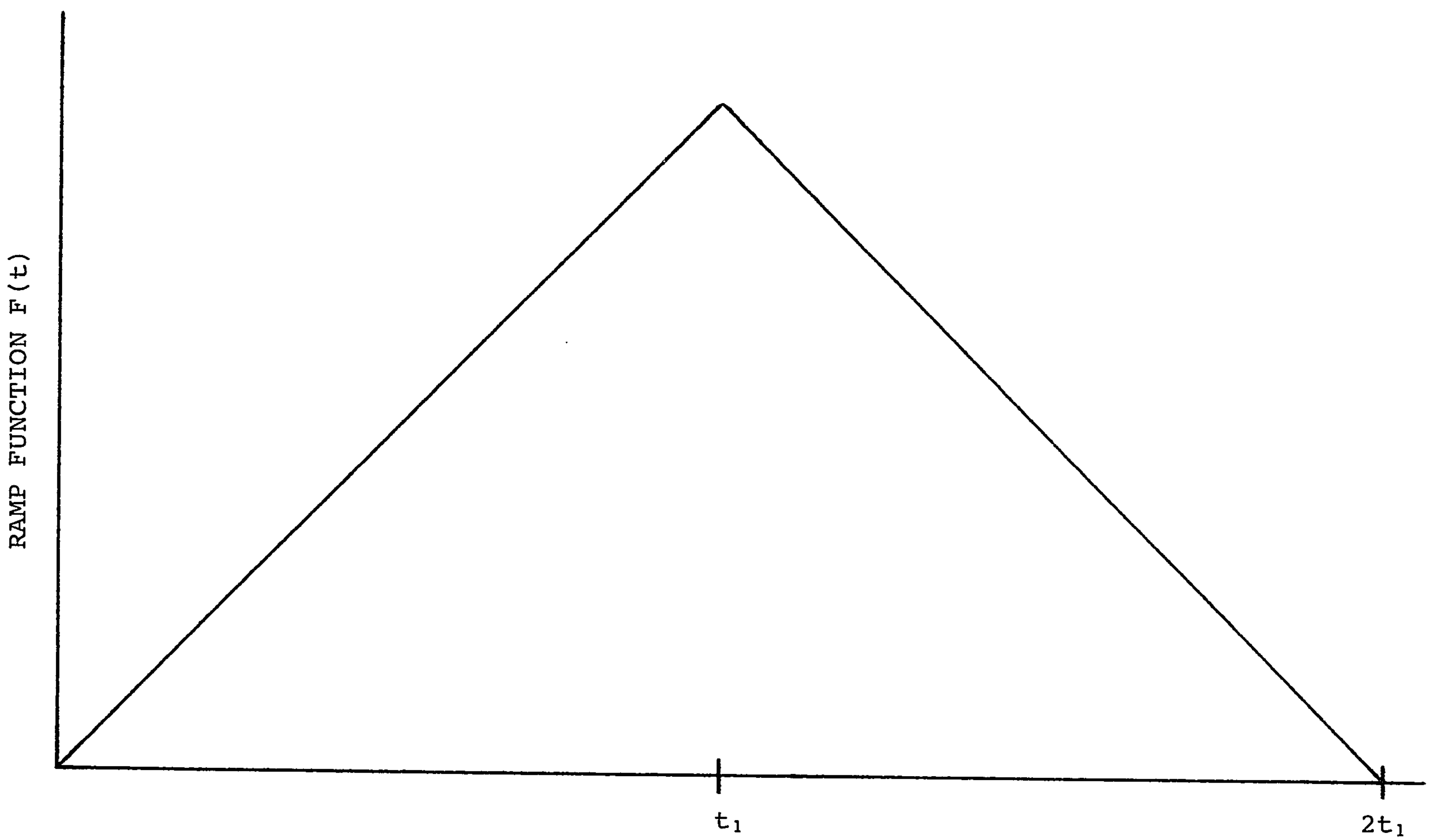

FIGURE 6: COUETTE VISCOMETER

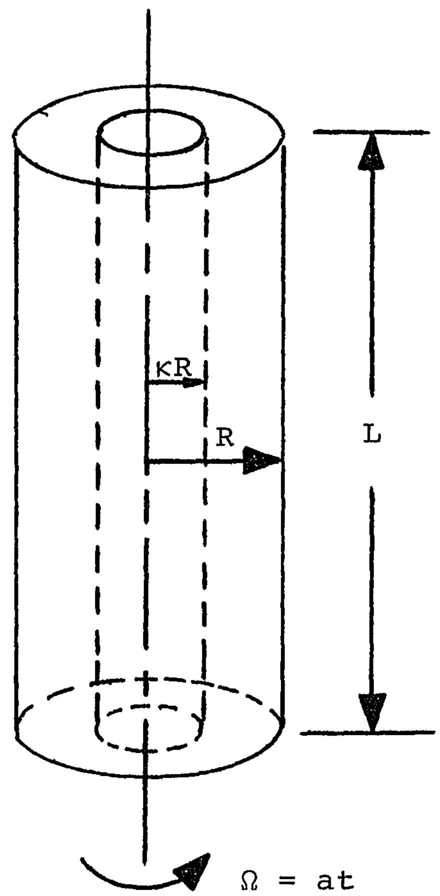

$$F(t) = aRt \; ; \; 0 \leq t \leq t_1 \qquad (4\text{-}22a)$$

$$F(t) = 2aRt_1 - aRt \; ; \; t_1 \leq t \leq 2t_1 \qquad (4\text{-}22b)$$

with a being the angular acceleration of the outer cylinder, and t_1 being the time required for the angular velocity of the outer cylinder to reach its maximum value. Since one of the boundary conditions is time-dependent, it is necessary to use Duhamel's Theorem (29) to obtain a solution to the equation of motion. According to Duhamel's Theorem, the velocity function in the angular direction may be obtained from the relationship

$$v_\theta(r,t) = \int_0^t F'(t - \xi)V(r,\xi)d\xi \qquad (4\text{-}23)$$

where F' is the time derivative of the time-dependent boundary condition and V is a velocity function in the angular direction which satifies the equation of motion with the following initial and boundary conditions

$$V(r,0) = 0 \qquad (4\text{-}24a)$$

$$V(\kappa R,t) = 0 \qquad (4\text{-}24b)$$

$$V(R,t) = 1 \qquad (4\text{-}24c)$$

Applying the method of separation of variables to the equation of motion subject to the above initial and boundary conditions, the velocity function V(r,t) becomes

$$V(r,t) = A_1\frac{r}{R} - A_2\frac{R}{r} + \sum_{i=1}^{\infty} E_i Z_1(\zeta\beta_i r)\exp[-\beta_i^2 t] \quad (4\text{-}25)$$

where the following simplifications have been introduced

$$A_1 = 1/(1 - \kappa^2) \quad (4\text{-}26a)$$

$$A_2 = \kappa^2/(1 - \kappa^2) \quad (4\text{-}26b)$$

$$\zeta = \sqrt{\rho/\mu} \quad (4\text{-}26c)$$

$$Z_1(\zeta\beta_i r) = J_1(\zeta\beta_i r)Y_1(\zeta\beta_i \kappa R) - Y_1(\zeta\beta_i r)J_1(\zeta\beta_i \kappa R)$$

(4-26d)

with J_1 and Y_1 being first order Bessel functions of the first and second kind, respectively. The combination function $Z_i(\zeta\beta_i r)$ was defined analogously to the combination function used in the paper by Bird and Curtiss. The eigenvalues β_i satisfy the relationship

$$J_1(\zeta\beta_i \kappa R)Y_1(\zeta\beta_i R) = J_1(\zeta\beta_i R)Y_1(\zeta\beta_i \kappa R) \quad (4\text{-}27)$$

The series constants E_i are obtained by means of a Sturm-Liouville analysis which yields the following expression for the E_i

$$E_i = \frac{\frac{A_1}{R}\left(R^2 Z_0(\zeta\beta_i R) - \kappa^2 R^2 Z_0(\zeta\beta_i \kappa R)\right) - A_2 R\left(Z_0(\zeta\beta_i R) - Z_0(\zeta\beta_i \kappa R)\right)}{\frac{1}{2}\zeta\beta_i\left(R^2 Z_0^2(\zeta\beta_i R) - \kappa^2 R^2 Z_0^2(\zeta\beta_i \kappa R)\right)} \tag{4-28}$$

Applying Duhamel's Theorem to the present situation, the angular velocity function becomes, when $0 \leq t \leq t_1$,

$$v_\theta(r,t) = a\left(A_1 r - A_2\frac{R^2}{r}\right)t + \sum_{i=1}^{\infty}\frac{aRE_i}{\beta_i^2}Z_1(\zeta\beta_i r)(1 - \exp[-\beta_i^2 t]) \tag{4-29a}$$

and when $t_1 \leq t \leq 2t_1$,

$$v_\theta(r,t) = a\left(A_1 r - A_2\frac{R^2}{r}\right)(2t_1 - t) \tag{4-29b}$$

$$+ \sum_{i=1}^{\infty}\frac{aRE_i}{\beta_i^2}Z_1(\zeta\beta_i r)(1 - 2\exp[-\beta_i^2 t_1] + \exp[-\beta_i^2 t])$$

Once the velocity function $v_\theta(r,t)$ has been determined, the shear stress distribution $\tau_{r\theta}(r,t)$ and the torque distribution $T(t)$ applied to the inner cylinder may be obtained from the relationships

$$\tau_{r\theta}(r,t) = -\mu r\frac{\partial}{\partial r}\left(v_\theta(r,t)/r\right) \tag{4-30}$$

$$T(t) = 2\pi\kappa^2 R^2 L\left(-\tau_{r\theta}(r,t)\right)_{r=\kappa R} \tag{4-31}$$

Therefore, when $0 \leq t \leq t_1$,

$$\tau_{r\theta}(r,t) = -\mu\left(\frac{2aA_2R^2t}{r^2} - \sum_{i=1}^{\infty}\frac{\zeta aRE_i}{\beta_i}Z_2(\zeta\beta_i r)(1 - \exp[-\beta_i^2 t])\right) \tag{4-32}$$

$$T(t) = 4\pi aLA_2R^2\mu t$$

$$+ 2\pi aL\kappa^2R^3\sqrt{\rho\mu}\left(\sum_{i=1}^{\infty}\frac{E_i}{\beta_i}Z_0(\zeta\beta_i\kappa R)(1 - \exp[-\beta_i^2 t])\right) \tag{4-33}$$

and for $t_1 \leq t \leq 2t_1$,

$$\tau_{r\theta}(r,t) = -\mu\left(\frac{2aA_2R^2}{r^2}(2t_1 - t)\right.$$

$$\left. - \sum_{i=1}^{\infty}\frac{\zeta aRE_i}{\beta_i}Z_2(\zeta\beta_i r)(1 - 2\exp[-\beta_i^2 t_1] + \exp[-\beta_i^2 t])\right) \tag{4-34}$$

$$T(t) = 4\pi aLR^2\mu A_2(2t_1 - t)$$

$$+ 2\pi aL\kappa^2R^3\sqrt{\rho\mu}\left(\sum_{i=1}^{\infty}\frac{E_i}{\beta_i}Z_0(\zeta\beta_i\kappa R)(1 - 2\exp[-\beta_i^2 t_1] + \exp[-\beta_i^2 t])\right) \tag{4-35}$$

Since both torque functions consist of two terms, we may express the torque function as

$$T(t) = T_1(t) + T_2(t) \tag{4-36}$$

where the functions $T_1(t)$ and $T_2(t)$ are defined by equations (4-33,4-35). Examination of these equations indicates that the function $T_1(t)$ is linear in time for both the upcurve and the downcurve of the flow curve. These equations also show that the function $T_2(t)$ represents a series of first order responses with diminishing amplitudes. Typical representations of these functions are shown in Figure 7. The total torque response function is the graphical sum of these two response functions. This graphical addition is shown in Figure 8. For a Newtonian fluid, the linear response function $T_1(t)$ represents the theoretically anticipated response of the shear stress under a ramp input shear rate. This indicates that $T_1(t)$ is the primary response function for a Newtonian fluid and that the first order response function $T_2(t)$ represents secondary responses of the shear stress under a ramp input shear rate. Therefore, these secondary responses must be responsible for the presence of any artificial hysteresis loops that may be observed. This analysis indicates that it is possible for a Newtonian fluid to exhibit non-Newtonian behavior under certain conditions.

Huang-Fabisiak Dimensionless Group

In order to minimize or eliminate the presence of any artificial non-Newtonian effects, it is necessary to demonstrate that these secondary responses are negligible with respect to the primary response function under the prevailing experimental conditions. This may be readily accomplished by the evaluation of a dimensionless quantity known as the Huang-Fabisiak number, N_{HF}. In order to evaluate this dimensionless group, it is necessary to rewrite the

FIGURE 7: RESPONSE FUNCTIONS

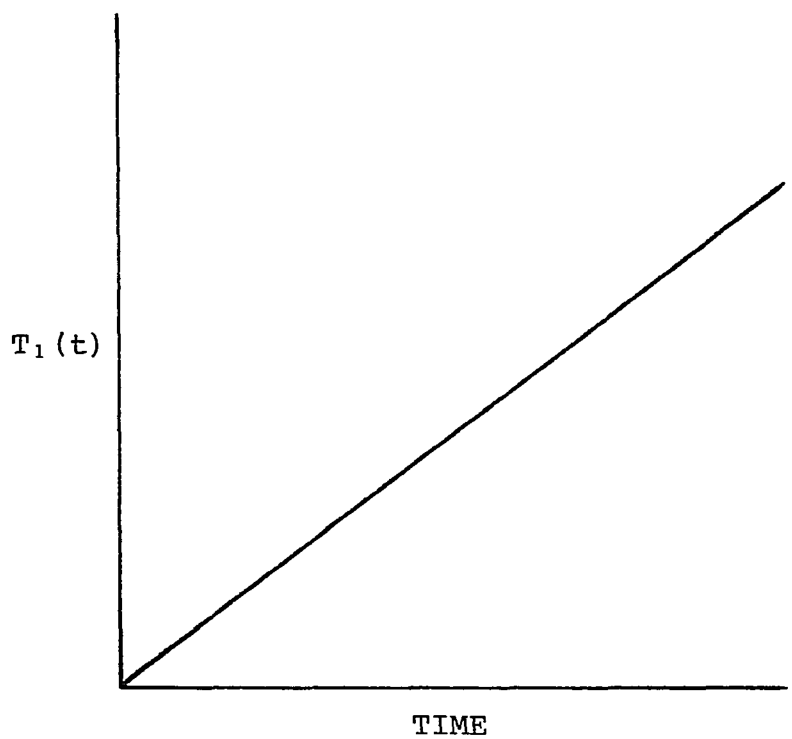

Linear Response Function

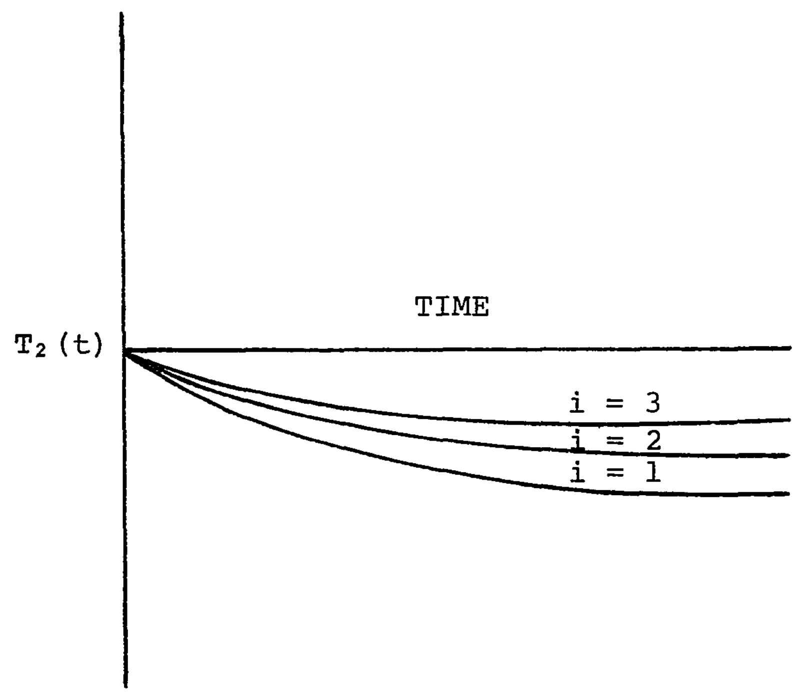

First Order Response Function

FIGURE 8: TOTAL TORQUE RESPONSE FUNCTIONS

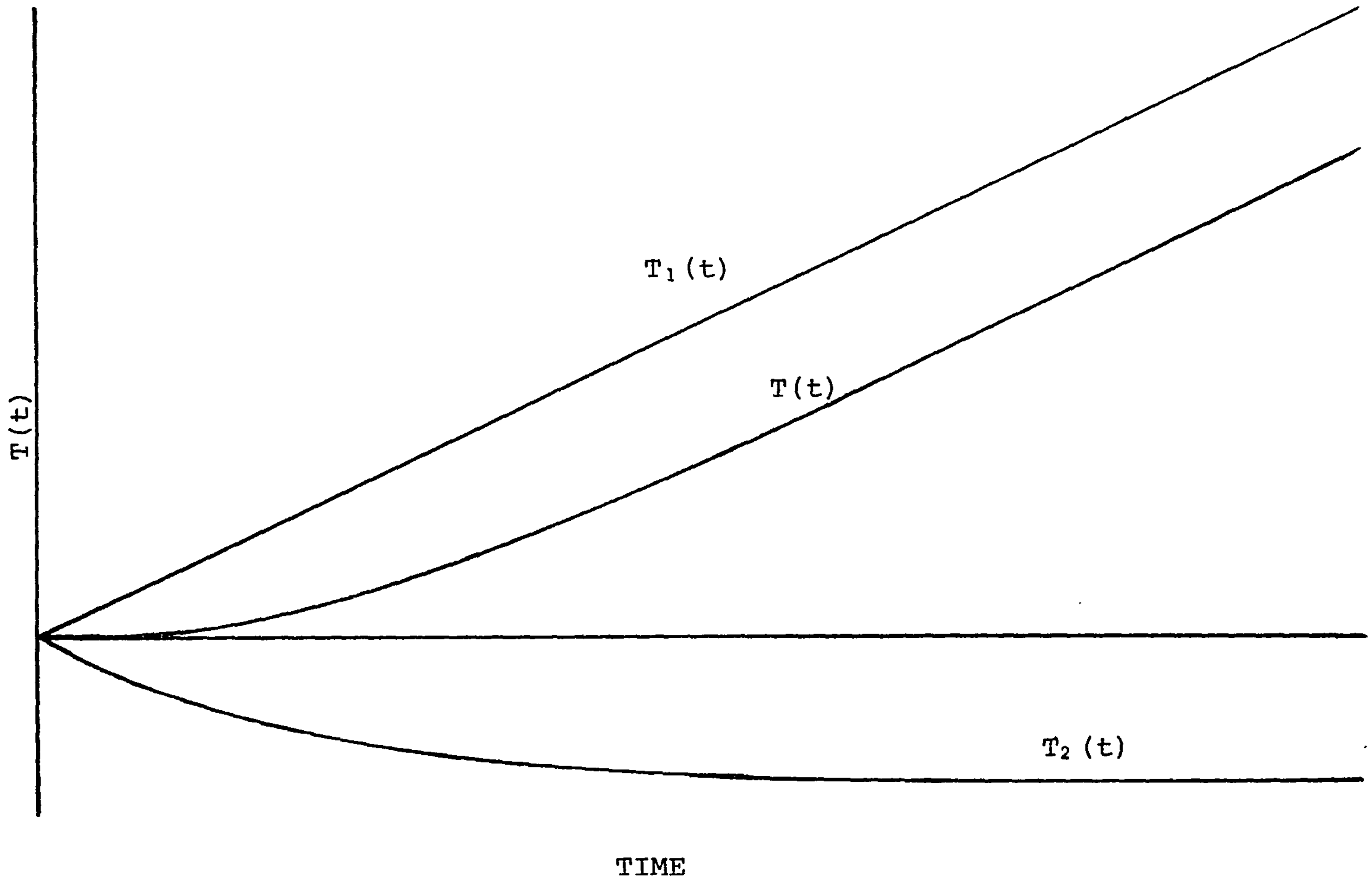

the total torque functions in a dimensionless form. Thus, equation (4-33) becomes

$$T^*(\sigma) = \sigma + \frac{(1 - \kappa^2)R\zeta}{2t_1}\left(\sum_{i=1}^{\infty} \frac{E_i}{\beta_i} Z_0(\zeta\beta_i\kappa R)(1 - \exp[-\beta_i^2 t_1\sigma])\right) \tag{4-37}$$

where the following dimensionless quantities have been defined

$$\sigma = t/t_1 \tag{4-38a}$$

$$T^*(\sigma) = \frac{(1 - \kappa^2)T(t)}{4\pi a L\kappa^2 R^2 \mu t} \tag{4-38b}$$

The quantity σ represents a dimensionless time and $T^*(\sigma)$ represents a dimensionless torque. Similarly, equation (4-35) becomes

$$T^*(\sigma) = (2 - \sigma) + \frac{(1 - \kappa^2)R\zeta}{2t_1}\left(\sum_{i=1}^{\infty} \frac{E_i}{\beta_i} Z_0(\zeta\beta_i\kappa R)\right.$$

$$\left.(1 - 2\exp[-\beta_i^2 t_1] + \exp[-\beta_i^2 t_1\sigma])\right) \tag{4-39}$$

The series portions of equations (4-37,4-39) are monotonic decreasing functions in total torque. The first term in these types of functions is usually the controlling term, such that the following dimensionless group, N_{HF}, defined as

$$N_{HF} = \frac{(1 - \kappa^2)R\zeta E_1 Z_0(\zeta\beta_1\kappa R)}{2t_1\beta_1} \tag{4-40}$$

may be considered as the controlling factor for the magnitude of the secondary responses for both the upcurve and downcurve of the flow curve. If this dimensionless group is small with respect to unity, then the experimentally observed rheological behavior is representative of the material being examined. Therefore, the dimensionless group, N_{HF}, may be used to detect the presence of any artificially generated hysteresis.

Shear Rate Determination

We have considered the different aspects of the shear stress response under a variety of different conditions. Exact solutions for the shear stress response under steady-state and transient conditions have been developed for a Newtonian fluid. Although the shear stress response can be readily obtained from the expressions for the total torque, the shear rate must be evaluated from the simultaneous solution of the equation of motion and the describing rheological equation of state. Kreiger and Maron (31) have proposed a method for the direct determination of the shear rate for a non-Newtonian fluid from concentric cylinder viscometric data. Their method requires that two sets of torque and angular velocity data be obtained from two different sets of cylinder radii. Kreiger and Elrod (32) have extended this method to yield a difference equation solution, which leads to a rapidly converging power series function of the radius ratio. Their error analysis demonstrated that only two terms of the power series are needed to approximate the sum of the series. Kreiger (33) has shown that certain forms of the infinite series which appear in the Kreiger and Elrod equations can be summed into a closed form, leading to an expression for the shear rate in which the dominant term is identical to the local power law approximation with appropriate correction terms being used to account for any deviation from power law behavior. As a consequence, the point by point application of the power law method is shown to give an excellent representation of the true shear rate in a concentric cylinder viscometer with a small and determinable error. Benis, Usami, and Chien (34) have discovered that using the mean shear rates determined from the equations for a Newtonian fluid were a reasonable approximation for the shear rates of human blood. They develop a simple technique of using the mean shear rates to determine the viscometric curve to within a few percent of that given by the power law relationship. Their method gives a relatively small error even for fluids whose behavior deviates markedly from that of a Newtonian fluid. The key parameter in the error minimization method is the radius ratio with the error diminishing as the two radii approached each other.

Recently, Huang (35) has developed a method to determine the shear rate for a fluid from a single set of torque and angular velocity data obtained from a concentric cylinder viscometer. If we consider the concentric cylinder viscometer displayed in Figure 6, we can use Huang's method to develop an exact expression for the determination of the shear rate for any fluid in a concentric cylinder arrangement. For the purpose of development, we will consider the case where the inner cylinder rotates with an angular velocity Ω, while a torque T is exerted on the outer cylinder which is stationary. For the steady-state flow of an incompressible fluid, the equation of motion reduces to

$$\frac{d}{dr}\left(r\tau_{r\theta}\right) = 0 \tag{4-41}$$

This equation may be integrated to give

$$\tau_{r\theta} = C/r^2 \tag{4-42}$$

The integration constant may be evaluated from the boundary condition

$$r = R; \ T = \left(2\pi r^2 L\tau_{r\theta}\right)_{r=R} \tag{4-43}$$

which gives

$$C = T/(2\pi L) \tag{4-44}$$

The shear stress distribution is now given by

$$\tau_{r\theta} = T/(2\pi L r^2) \tag{4-45}$$

For time-independent, incompressible fluids, either Newtonian or non-Newtonian, the shear stress - shear rate functional relationship may be expressed by the generalized rheological equation

$$\tau_{r\theta} = -\eta\dot{\gamma}_{r\theta} = -\eta r\left[\frac{d}{dr}(v_\theta/r)\right] \qquad (4\text{-}46)$$

where η, if the fluid is non-Newtonian, is an invariant function of the shear stress or shear rate tensor. Assuming that the angular velocity is a continuous function of the radius in the interval $\kappa R \leq r \leq R$, subject to the boundary condition

$$r = R;\ v_\theta = 0 \qquad (4\text{-}47)$$

we may express the angular velocity distribution as

$$\frac{v_\theta}{r} = \int_R^r \frac{d(v_\theta)}{dr}\, dr \qquad (4\text{-}48)$$

Using equation (4-46), the integrand of equation (4-48) may be alternatively expressed in terms of the shear rate as

$$v_\theta/r = \int_R^r \dot{\gamma}_{r\theta}\, \frac{dr}{r} \qquad (4\text{-}49)$$

Differentiation of the shear stress distribution with respect to r yields

$$d\left(\tau_{r\theta}\right)/dr = -T/(\pi L r^2) \qquad (4\text{-}50)$$

Using the shear stress distribution to make a change of variable, we can rewrite equation (4-49) as

$$v_\theta/r = -\int_{\tau_{r\theta}(R)}^{\tau_{r\theta}(r)} \dot{\gamma}_{r\theta} \frac{d\tau_{r\theta}}{2\tau_{r\theta}} \tag{4-51}$$

The specific integration limits now become

$$r = \kappa R;\ \left(\tau_{r\theta}\right)_{r=\kappa R} = T/(2\pi L\kappa^2 R^2);\ \left(v_\theta/r\right)_{r=\kappa R} = \Omega \tag{4-52a}$$

$$r = R;\ \left(\tau_{r\theta}\right)_{r=R} = T/(2\pi L R^2);\ \left(v_\theta/r\right)_{r=R} = 0 \tag{4-52b}$$

Equation (4-51) now becomes

$$\Omega = -\int_{T/(2\pi L R^2)}^{T/(2\pi L\kappa^2 R^2)} \dot{\gamma}_{r\theta} \frac{d\tau_{r\theta}}{2\tau_{r\theta}} \tag{4-53}$$

Assuming that the integrand is analytic with respect to $\tau_{r\theta}$ and T, and that the partial derivatives with respect to T of both integration limits exist, the integral equation may be differentiated with respect to T to give

$$\frac{d\Omega}{dT} = \left(\frac{\dot{\gamma}_{r\theta}}{2\tau_{r\theta}}\right)_{r=R} [1/(2\pi L R^2)] - \left(\frac{\dot{\gamma}_{r\theta}}{2\tau_{r\theta}}\right)_{r=\kappa R} [1/(2\pi L\kappa^2 R^2)] \tag{4-54}$$

which can be simplified to give

$$2T\frac{d\Omega}{dT} = \left(\dot{\gamma}_{r\theta}\right)_{r=R} - \left(\dot{\gamma}_{r\theta}\right)_{r=\kappa R} \tag{4-55}$$

In general, the shear rate may be expressed as a unique function of the shear stress

$$\dot{\gamma}_{r\theta} = f(\tau_{r\theta}) \tag{4-56}$$

Using equation (4-45), we may replace this functional relationship with

$$f(\tau_{r\theta}) = G(T/r^2) \tag{4-57}$$

which now may be incorporated into equation (4-55) to give

$$2T(d\Omega/dT) = G_2(T/R^2) - G_1(T/\kappa^2R^2) \tag{4-58}$$

where $G_2(T/R^2)$ and $G_1(T/\kappa^2R^2)$ are the shear rate functions evaluated at $r=R$ and $r=\kappa R$, respectively. The left-hand side of equation (4-58) may be evaluated from a set of torque and angular velocity data. Therefore, a unique shear rate function may be determined accordingly for any material.

If the fluid is a simple Newtonian, the shear rate function is given by

$$\dot{\gamma}_{r\theta} = -(\tau_{r\theta}/\mu) = T/(2\pi\mu Lr^2) \tag{4-59}$$

and equation (4-58) becomes

$$d\Omega/dT = [1/(4\pi\mu L)][1/(\kappa^2R^2) - 1/R^2] \qquad (4\text{-}60)$$

which represents a simple linear relationship between the torque and the angular velocity.

If the rheological equation of state is unknown, as is the usual case, the shear rate expression may be estimated with a general polynomial expression of the form

$$\dot{\gamma}_{r\theta} = \lambda_0 + \lambda_1\tau_{r\theta} + \lambda_2\tau_{r\theta}^2 + \cdots + \lambda_N\tau_{r\theta}^N = \sum_{i=0}^{N} \lambda_i\tau_{i\theta}^i \qquad (4\text{-}61)$$

where the λ_i are regression constants to be determined from an analysis of the torque and angular velocity data. Substitution of this polynomial expression into equation (4-58) gives

$$2T\frac{d\Omega}{dT} = \sum_{i=0}^{N} \left(\frac{\kappa^2 - 1}{2\pi L\kappa^2R^2}\right)^i \lambda_i T^i \qquad (4\text{-}62)$$

Using any of the conventional regression techniques available, the regression constants λ_i may be evaluated. Once they have been determined, the shear rate may be evaluated.

Although this method proposes an exact method for the determination of the shear rate, it has its drawback in that an experiment may not be performed at a pre-determined shear rate. Most experimental studies are performed using an apparent shear rate which is determined from the equations for a Newtonian fluid. This approach enables the determination of the shear rate range prior to the actual taking of the experimental data. In reality, this approach is a reasonable approximation for most fluids whose behavior is not too markedly different from that of a Newtonian fluid. Since all of the available data on blood rheology is reported using the apparent shear rate, this approach will be used to provide a means of comparison with existing data and to conform to current practice.

RESULTS

TABLE I: HEMATOLOGICAL PARAMETERS

Parameter	Sample	N	$\overline{X}$	S D	P
Hemoglobin (gm%)	Normal	16	14.80	1.29	-
	Polycythemia	11	17.47	1.22	<0.001
	Parkinson's	10	14.85	1.01	>0.900
	Hypertension	8	14.38	1.49	0.502
Hematocrit (%)	Normal	16	44.75	4.07	-
	Polycythemia	11	54.13	4.28	<0.001
	Parkinson's	10	43.24	2.19	0.311
	Hypertension	8	43.75	4.29	0.600
Red Blood Cell Count ($10^6/mm^3$)	Normal	16	4.496	0.782	-
	Polycythemia	11	5.690	0.865	0.002
	Parkinson's	10	5.082	0.494	0.054
	Hypertension	8	4.653	0.605	0.639
Fibrinogen (mg/100ml)	Normal	16	203.4	58.2	-
	Polycythemia	11	277.1	95.7	0.027
	Parkinson's	10	269.5	32.3	0.007
	Hypertension	8	270.6	62.6	0.021
Total Protein (gm/dl)	Normal	16	7.100	0.487	-
	Polycythemia	11	7.245	0.587	0.508
	Parkinson's	10	7.400	0.249	0.097
	Hypertension	8	7.438	0.343	0.109
Albumin (gm/dl)	Normal	16	4.241	0.381	-
	Polycythemia	11	4.025	0.302	0.150
	Parkinson's	10	4.420	0.140	0.118
	Hypertension	8	3.975	0.286	0.112

TABLE I: CONT'D.

Parameter	Sample	N	$\overline{X}$	S D	P
α_1-Globulin (gm/dl)	Normal	15	0.205	0.118	-
	Polycythemia	11	0.226	0.074	0.622
	Parkinson's	10	0.190	0.030	0.655
	Hypertension	8	0.150	0.050	0.246
α_2-Globulin (gm/dl)	Normal	15	0.624	0.113	-
	Polycythemia	11	0.710	0.149	0.126
	Parkinson's	10	0.790	0.130	0.006
	Hypertension	8	0.725	0.120	0.074
β-Globulin (gm/dl)	Normal	15	0.877	0.114	-
	Polycythemia	11	0.939	0.120	0.212
	Parkinson's	10	1.020	0.154	0.017
	Hypertension	8	1.150	0.180	<0.001
γ-Globulin (gm/dl)	Normal	15	1.123	0.349	-
	Polycythemia	11	1.394	0.359	0.079
	Parkinson's	10	1.010	0.192	0.381
	Hypertension	8	1.463	0.328	0.044
Cholesterol (mg/dl)	Normal	16	169.8	45.1	-
	Polycythemia	11	207.9	77.0	0.161
	Parkinson's	10	216.3	24.0	0.009
	Hypertension	8	210.4	47.6	0.067
Triglyceride (mg/dl)	Normal	16	88.1	39.0	-
	Polycythemia	11	160.2	84.3	0.009
	Parkinson's	10	119.9	32.0	0.049
	Hypertension	8	139.4	72.4	0.044

TABLE II: RHEOLOGICAL PARAMETERS

Parameter	Sample	N	$\bar{X}$	S D	P
τ_0 ($\frac{dyne}{cm^2}$)	Normal	16	0.1618	0.0578	-
	Polycythemia	11	0.3112	0.0706	0.001
	Parkinson's	10	0.1388	0.0303	0.278
	Hypertension	8	0.2075	0.1038	0.200
μ (Poise)	Normal	16	0.1051	0.0140	-
	Polycythemia	11	0.1650	0.0320	0.001
	Parkinson's	10	0.1077	0.0124	0.649
	Hypertension	8	0.1243	0.0325	0.688
c_1 (sec^{n-1})	Normal	16	0.1451	0.0324	-
	Polycythemia	11	0.1182	0.0216	0.038
	Parkinson's	10	0.1561	0.0210	0.365
	Hypertension	8	0.1228	0.0185	0.092
A (Poise)	Normal	16	0.4063	0.1003	-
	Polycythemia	11	0.7075	0.2052	0.001
	Parkinson's	10	0.5188	0.1109	0.018
	Hypertension	8	0.6478	0.3237	0.070
n (dimension-less)	Normal	16	1.6017	0.2193	-
	Polycythemia	11	1.7046	0.1180	0.287
	Parkinson's	10	1.4553	0.1723	0.098
	Hypertension	8	1.6379	0.3562	0.772
η (Poise)	Normal	16	0.1631	0.0339	-
	Polycythemia	11	0.2772	0.0568	0.001
	Parkinson's	10	0.1724	0.0285	0.495
	Hypertension	8	0.2135	0.0880	0.164
$\eta - \mu$ (Poise)	Normal	16	0.0580	0.0223	-
	Polycythemia	11	0.1123	0.0279	0.001
	Parkinson's	10	0.0647	0.0186	0.455
	Hypertension	8	0.0893	0.0579	0.184

TABLE III: HCRF HEMATOLOGICAL PARAMETERS

Parameter	Sample	N	$\overline{X}$	S D	P
AGE (years)	Normals	13	27.9	7.2	-
	HCRF	77	46.6	5.5	-
	I	15	46.0	4.5	-
	II	5	48.6	4.5	-
	III	6	50.5	2.9	-
	I,II	15	45.0	5.5	-
	I,III	14	44.7	5.6	-
	II,III	13	48.7	5.6	-
	I,II,III	9	46.7	6.0	-
CIGARETTES PER DAY	Normals	13	N.A.	N.A.	N.A.
	HCRF	53	35.2	14.4	-
	I	15	38.0	10.0	-
	II	5	0.0	0.0	-
	III	6	0.0	0.0	-
	I,II	15	36.3	9.6	-
	I,III	14	37.0	20.0	-
	II,III	13	0.0	0.0	-
	I,II,III	9	26.1	13.1	-
HEMATOCRIT (%)	Normals	13	46.4	2.3	-
	HCRF	75	46.6	3.2	0.834
	I	15	47.4	3.0	0.357
	II	5	45.4	4.0	0.543
	III	6	45.2	1.9	0.307
	I,II	14	45.8	3.0	0.582
	I,III	14	46.9	3.0	0.647
	II,III	12	46.1	2.6	0.772
	I,II,III	9	48.7	3.8	0.111

TABLE III: CONT'D.

Parameter	Sample	N	$\overline{X}$	S D	P
DIASTOLIC BLOOD PRESSURE (mm Hg)	Normals	13	N.A.	N.A.	-
	HCRF	77	90.8	10.5	-
	I	15	83.1	4.1	-
	II	5	104.2	8.2	-
	III	6	83.2	4.1	-
	I,II	15	98.8	4.6	-
	I,III	14	78.9	5.7	-
	II,III	13	100.0	6.2	-
	I,II,III	9	94.6	4.4	-
CHOLES-TEROL (mg/dl)	Normals	13	168.2	49.2	-
	HCRF	72	256.0	42.0	<0.001
	I	13	220.4	17.2	0.004
	II	5	230.4	5.8	0.018
	III	6	299.3	38.9	<0.001
	I,II	12	209.8	25.3	0.019
	I,III	14	289.1	32.1	<0.001
	II,III	13	275.8	20.9	<0.001
	I,II,III	9	274.0	25.8	<0.001
TRIGLYCER-IDE (mg/dl)	Normals	13	87.2	28.9	-
	HCRF	70	194.0	101.9	<0.001
	I	11	154.4	54.0	0.002
	II	5	280.3	210.9	0.009
	III	6	164.0	34.2	<0.001
	I,II	12	172.3	54.1	<0.001
	I,III	14	225.4	90.5	<0.001
	II,III	13	202.7	108.7	0.003
	I,II,III	9	181.9	94.2	0.006

TABLE IV; HCRF RHEOLOGICAL PARAMETERS

Parameter	Sample	N	$\overline{X}$	S D	P
	Normals	13	0.167	0.049	-
	HCRF	78	0.205	0.057	0.020
	I	15	0.217	0.072	0.053
	II	5	0.199	0.038	0.236
τ_0	III	6	0.160	0.030	0.764
($dyne/cm^2$)	I,II	15	0.191	0.037	0.173
	I,III	14	0.218	0.058	0.028
	II,III	12	0.227	0.055	0.011
	I,II,III	9	0.207	0.056	0.108
	Normals	13	0.109	0.012	-
	HCRF	78	0.133	0.021	<0.001
	I	15	0.135	0.022	0.001
	II	5	0.137	0.012	<0.001
μ	III	6	0.118	0.012	0.174
(Poise)	I,II	15	0.128	0.014	0.001
	I,III	14	0.137	0.027	0.005
	II,III	12	0.138	0.018	0.001
	I,II,III	9	0.135	0.022	0.005
	Normals	13	0.143	0.032	-
	HCRF	78	0.141	0.029	0.823
	I	15	0.137	0.034	0.650
	II	5	0.148	0.011	0.752
c_1 (sec^{n-1})	III	6	0.154	0.021	0.478
	I,II	15	0.145	0.028	0.867
	I,III	14	0.146	0.029	0.808
	II,III	12	0.130	0.022	0.275
	I,II,III	9	0.128	0.035	0.335

TABLE IV: CONT'D.

Parameter	Sample	N	$\overline{X}$	S. D	P
A (Poise)	Normals	13	0.409	0.091	-
	HCRF	78	0.544	0.124	<0.001
	I	15	0.532	0.116	0.008
	II	5	0.605	0.101	0.003
	III	6	0.543	0.142	0.035
	I,II	15	0.548	0.084	<0.001
	I,III	14	0.552	0.159	0.012
	II,III	12	0.554	0.098	0.002
	I,II,III	9	0.521	0.148	0.050
n	Normals	13	1.616	0.241	-
	HCRF	78	1.561	0.251	0.471
	I	15	1.627	0.159	0.891
	II	5	1.365	0.321	0.113
	III	6	1.371	0.204	0.059
	I,II	15	1.482	0.161	0.105
	I,III	14	1.607	0.284	>0.900
	II,III	12	1.588	0.223	0.775
	I,II,III	9	1.702	0.307	0.492
η (Poise)	Normals	13	0.171	0.032	-
	HCRF	78	0.209	0.041	0.004
	I	15	0.216	0.051	0.014
	II	5	0.212	0.023	0.028
	III	6	0.182	0.023	0.484
	I,II	15	0.199	0.025	0.019
	I,III	14	0.217	0.047	0.010
	II,III	12	0.223	0.032	<0.001
	I,II,III	9	0.209	0.044	0.044

TABLE IV: CONT'D.

Parameter	Sample	N	$\overline{X}$	S D	P
	Normals	13	0.062	0.022	-
	HCRF	78	0.076	0.022	0.041
	I	15	0.081	0.030	0.084
	II	5	0.075	0.017	0.280
$\eta - \mu$	III	6	0.064	0.014	0.850
(Poise)	I,II	15	0.072	0.012	0.162
	I,III	14	0.080	0.021	0.048
	II,III	12	0.084	0.017	0.015
	I,II,III	9	0.073	0.023	0.294

TABLE V: N_{HF} DETERMINATIONS

Case I	Case II
$R = 1.60$ cm	$R = 1.60$ cm
$\rho = 1.06$ g/cm^3	$\rho = 1.06$ g/cm^3
$\mu = 0.10$ Poise	$\mu = 0.20$ Poise
$\kappa = 0.95$	$\kappa = 0.95$
$N_{HF} = -0.000862$	$N_{HF} = -0.000427$
$t_1 = 10$ sec	$t_1 = 10$ sec

DISCUSSION

Rheological determinations and standard clinical hematological evaluations were performed on sixteen normal subjects and compared to similar data obtained from persons suffering from polycythemia, Parkinsonism, or hypertension. All of the subjects were participants in selected clinical pharmacological studies with the normals serving as the control group for the clinical investigations. Polycythemia is a physiological disorder characterized by an unusually large number of red blood cells being present in the blood. Parkinsonism is a neurological disorder characterized by a rigidity of the musculature in either widespread or isolated areas of the body, tremors at rest in the involved areas, and a loss of involuntary and associated movements. Hypertension refers to a physiological condition in which the human blood pressure is unusually elevated. Adults are considered to be normotensive if their systolic blood pressure is between 120 and 140 mm Hg and their diastolic blood pressure is between 70 and 90 mm Hg. There is considerable controversy as to where to draw the line of demarcation between normal and elevated blood pressure, and both systolic and diastolic blood pressures rise with age in apparently healthy humans.

It was intended in this aspect of the study to establish values for certain rheological parameters for healthy individuals and to compare them to those values of persons undergoing treatment for known physiological disorders. The investigative emphasis was placed on the identification and examination of any correlations between physiological and rheological parameters. All subjects in this aspect of the study of the rheological behavior of human blood were participants in a series of ongoing clinical pharmacological investigations administered by the Special Treatment Unit of Beth Israel Medical Center in Newark, New Jersey. The Center supplied blood samples for the rheological testing along with the subject category, age, sex, and blood chemistry evaluations. Specific medical information was not supplied and group determinations were made by the Center according to their established criteria. The control group consisted of thirteen males and three females having an average age of 28.3 ± 6.7 and were considered to be normal healthy adults according to contemporary medical standards. The polycythemia group consisted of nine males and two females having an average age of 64.4 ± 6.9. The Parkinsonism group consisted of seven males and three females having an average age of 61.8 ± 6.9, and the hypertensive group consisted of three males and five females having an average age of 55.4 ± 8.4.

Clinical determinations performed on the various participants in this aspect of the study are summarized in Table I. The average parameter values along with their respective standard deviations are listed for all the biophysical determinations made during this study. Data analysis for all of the groups was performed on the sample means using the Student t-test for small sample sizes, and the standard F-test was used for the analysis of variance. A 95% confidence limit was used in the F-test evaluations. The P parameter entered in the tables represents the probability that the observed difference between the sample mean and the control mean is due to random chance. This method of sample comparison is commonly employed in biomedical investigations and was used in this study to maintain consistency with existing literature results. The difference between means was considered to be statistically significant when the probability parameter was less than 0.05. Any value of P that is larger than 0.05 increases the probability that any observed difference in the sample means is due to sampling variations.

Examination of the results in Table I indicates that the polycythemia group displayed different parameter values for hematocrit, hemoglobin, red blood cell count, triglyceride, and fibrinogen. The Parkinsonism group displayed different parameter values for fibrinogen, serum cholesterol, α_2-globulin, and β-globulin. The hypertensive group displayed different values for fibrinogen, β-globulin, and γ-globulin.

Rheological determinations performed on these samples are summarized in Table II. As shown in Table II, the polycythemia group displayed different values for the yield stress, Newtonian viscosity contribution, kinetic rate constant, equilibrium value of the structural arrangement parameter, steady-state viscosity, and the non-Newtonian viscosity contribution. These differences are not surprising considering the abnormal levels of hematrocrit, hemoglobin, fibrinogen, and red blood cell count exhibited by the polycythemia. An increase in the blood viscosity has been traditionally observed in cases of polycythemia and variations in the rheological parameters were anticipated. There was no statistical difference observed in order of the breakdown reaction of rouleaux to individual cells. Coincidentally, there was no difference in this parameter for any of the groups under investigation. Apparently, the breakdown reaction mechanism is similar for all of the groups in question. The Parkinsonism group only displayed a different value for the structural arrangement parameter. The higher value of the parameter indicates that a higher level of rouleaux aggregation is present, but the significance of this is unknown at present. Ironically, the hypertensives did not display any differences in rheological parameters, although it must be noted that the type of hypertension that the group was being treated for is referred to as essential hypertension, indicating that it is of unknown physiological origin.

Considering the relatively small sample sizes used in this aspect of the study, it would appear to be more appropriate to make qualitative, rather than quantitative, inferences from these results. It is evident that a hematological disorder, such as polycythemia, will have distinct effects upon the rheological behavior of human blood and that these effects may be characterized in terms of rheological paramaters. Based on the results from the essential hypertension and Parkinsonism groups, non-hematological disorders might not affect the rheological behavior of blood to an appreciable extent, as only slight parameter variations were detected. It is also quite possible that the therapeutic agents administered to these patients relieved the physiological symptoms, which in turn could correct any rheological abnormalities.

The next aspect of this investigation was the examination of the rheological model as a predictive or diagnostic tool as applied to the rheological behavior of apparently healthy adult males who had exhibited elevated levels of one or more of the following coronary risk factors: cigarette smoking, serum cholesterol, and diastolic blood pressure. These risk factors are well documented in the medical literature as being commonly associated with a high incidence of coronary heart disease (CHD). Blood samples and risk factor levels for seventy-eight adult males were supplied by St. Michael's Medical Center (Newark, NJ). The coronary risk factor levels used in this study were: (a) any level of cigarette smoking, (b) serum cholesterol of greater than 260 mg/dl, and (c) a diastolic blood pressure of greater than 90 mm Hg. All of the subjects were free of CHD, but were considered to be at an elevated level of risk of coronary heart disease using contemporary medical standards. Biophysical data for the high coronary risk factor (HCRF) subjects are given in Table III along with similar data for a group of thirteen normal adult males who served as a control for this study. The HCRF group was subdivided into groups according to the presence of one or more risk factors.

Group I included only cigarette smokers; group II included only hypertensives; and group III included only those with elevated serum cholesterol. The remaining groups consisted of subjects possessing any of the possible combinations of two or more risk factors. The rationale behind this subdivision process was to explore and identify the existence of any synergistic risk factor effects in terms of alterations in rheological parameters. Rheological parameter values for the HCRF and control groups are given in Table IV. The HCRF group displayed significantly different parameter values for the yield stress, the Newtonian viscosity contribution, the equilibrium value of the structural arrangement parameter, the steady-state viscosity, and the non-Newtonian viscosity contribution. These results indicate that an elevation in the levels of HCRF will result in an adverse alteration of the rheological behavior of a subject's blood. The obvious implication is that rheological screening has a potential use as a diagnostic tool for cardiovascular disorders. The results seem plausible considering that an elevation in the blood viscosity would tend to increase the workload of the circulatory system and place an increased strain on the heart. Although a subject may have outward signs of good cardiovascular health, the rheological behavior of his/her blood may indicate the onset of an unhealthy state before physical symptoms become evident.

The final phase of this investigation dealt with the examination of the possibility of the occurrence of artificially created hysteresis loops. Since hysteresis loop analysis is an integral part of the rheological analysis of the thixotropic phenomena exhibited by human blood, it is essential to eliminate or minimize any background or artifact effects of the testing procedure. In essence, it is desirable to identify the conditions under which it would be possible for a known material to exhibit abnormal properties. For this investigation, the basic premise was that the observed hysteresis loop behavior was characteristic of the blood sample and not artificially generated. In order to examine the possibility of a non-thixotropic material generating hysteresis loops, the mathematical development of the Couette viscometer equations under the conditions of a ramp function angular velocity were examined. Analysis of the solution indicates that it is mathematically possible for a Newtonian fluid to exhibit hysteresis loop behavior under certain experimental conditions. The site and shape of the artificial hysteresis loop is controlled by the magnitude of a dimensionless group. The relative magnitude of the dimensionless group, N_{HF}, was examined for two cases which were representative of the range of experimental conditions under which the thixotropic behavior of human blood was investigated. The viscosity was the variable of interest in the parameter sensitivity investigation since the Couette dimensions were fixed and the sample densities were essentially constant. Since most of the blood samples tested possessed an apparent viscosity of between 0.1 and 0.2 poise, it was felt that these two cases would be sufficiently representative. The case results are given in Table V.

For both sets of conditions, the magnitude of the dimensionless group was small with respect to unity and indicated that a Newtonian fluid, under the prevailing experimental conditions, would not generate an artificial hysteresis loop. Therefore, any hysteresis loop observed under these conditions must be attributed to the thixotropic nature of the material being examined. Thus, the hysteresis loop behavior observed is a direct result of the thixotropy of human blood.

This dimensionless group may be used to determine the relative magnitude of the secondary responses that are present during any set of experimental conditions. In this investigation, the dimensionless group was used in the analysis of the thixotropy of human blood. This analysis is not restricted to human blood, but may be applied to any thixotropic material to insure that any hysteresis loop behavior is a result of the thixotropic nature of the material being investigated.

CONCLUSIONS

Whole human blood is a thixotropic fluid whose apparent viscosity is a function of the rate and duration of shear. The thixotropic behavior of human blood is demonstrated by the experimental occurrence of both hysteresis loop and torque-decay flow curves during the rheological testing of a blood sample. This thixotropic behavior can be characterized by means of the Huang rheological model and an analysis of the various model parameters can provide a quantitative comparison among blood samples from different subjects. The representation of the rheological behavior of human blood using thixotropic parameters is superior to the use of apparent viscosity data taken at different shear rates. These thixotropic parameters can be correlated with various biophysical parameters and used as a diagnostic or monitoring method. These correlations could provide new information about how the chemical constituents of the blood affect its rheological behavior which, in turn, could eventually alter the circulatory behavior of blood in the tested individual.

It is possible to establish a range and distribution for each parameter by testing the blood of apparently healthy subjects as was demonstrated in this study. These parameter values can then be compared with those values obtained from subjects suffering from known physiological disorders. This was demonstrated using patients being treated for either polycythemia, Parkinsonism, or essential hypertension. Only the polycythemia group displayed markedly abnormal values for some of the parameter values. This result was not unexpected, as polycythemia is a hematological disorder which has limited specific treatment such as phlebotomy and hemodilution. The Parkinsonism and essential hypertension groups displayed minimal, abnormal rheological behavior. The possible explanations for this are that these disorders do not directly affect the rheological behavior of blood to an appreciable extent or the pharmacological therapy being administered relieves both physiological and rheological symptoms. The potential interrelationship between pharmacological treatment and rheological behavior presents an interesting area for future investigations.

The detection of abnormalities in any of the thixotropic parameters may be a warning signal for the onset of a pathological disorder. Alterations in the rheological behavior of blood cannot be predicted from measured hematological parameters. Rheological properties appear to be a sensitive reflection of microcirculatory events based upon the Huang model. Thus, the analysis of rheological parameters may provide a means to assess the alterations that exist in microcirculatory flow functions and define the pathophysiology that exists within the microcirculation during altered hemodynamic states. The diagnostic potential of rheological screening was demonstrated in the analysis of apparently healthy adult males having elevated levels of coronary risk factors. There were distinct alterations in the thixotropic parameters of these subjects and these alterations could be an indication of potential circulatory or cardiovascular distress. These results indicate the diagnostic potential of rheological screening with respect to various circulatory and cardiovascular disorders.

A mathematical analysis of the equations of change for the experimental system indicated that it is possible to observe artificially created hysteresis loops under certain experimental conditions. The size and shape of any artificially created hysteresis loop is controlled by the relative magnitude of a dimensionless group designated as N_{HF}. This dimensionless group may be used to detect and eliminate the presence of any secondary effects which would mask the actual rheological behavior of the material being investigated.

RECOMMENDATIONS

1.) Parameter sensitivity studies should be continued to completely determine the functional relationship between thixotropic parameters and hematological parameters.

2.) The experimental equipment should be further modified to enable temperature sensitivity studies to be performed on blood samples. These studies should reveal what alterations in rheological behavior could occur under extreme body temperature changes either pathologically or artificially induced.

3.) Experimental studies should be initiated to examine the effects of pharmacological agents on the rheological behavior of blood. Of particular interest would be the various cardiovascular and circulatory medications.

4.) Specific hematological disorders, such as sickle-cell anemia, should be investigated. Altered rheological behavior could be used to evaluate potential treatments for these disorders.

5.) The thixotropic model needs to be expanded to explicitly contain temperature and composition functions. This would extend the model's capabilities.

6.) Attempts should be made to improve the sensitivity of the experimental apparatus such that even minute alterations in rheological behavior could be detected.

APPENDIX A

EXPERIMENTAL

All rheological testing was performed using a modified Weissenberg Rheogoniometer. The original motor was replaced by an electronically driven stepping motor, which is capable of delivering a continuously variable speed for generating the ramp and step function inputs for the shear rate. A block diagram of the modified instrumentation is shown in Figure 9. A pulse generating control panel was connected to the stepping motor. This arrangement can provide a continuously linear or constant speed drive of the Rheogoniometer. The test cell was a specially designed double Couette. The torque output signal was transmitted by a transducer and simultaneously recorded with the input signal of the control panel. The input signal was either the angular velocity or time. The blood samples were well mixed prior to their being introduced into the cell. All measurements were made at a room temperature of 22 ± 1 ^{o}C.

The operating conditions for generating the flow curve were a time (t_1) of 10 (sec) for the shear rate to reach its maximum value ($\dot{\gamma}_m$) using a value of 0.766 $(\text{sec})^{-2}$ for the proportionality constant (α) for the shear rate input. In generating the torque-decay curve, the constant shear rate ($\dot{\gamma}_c$) was maintained at 3.066 $(\text{sec})^{-1}$. These operating parameters were determined experimentally. The operating conditions are chosen such that an optimal observance of the thixotropic behavior is possible. These operating condi-

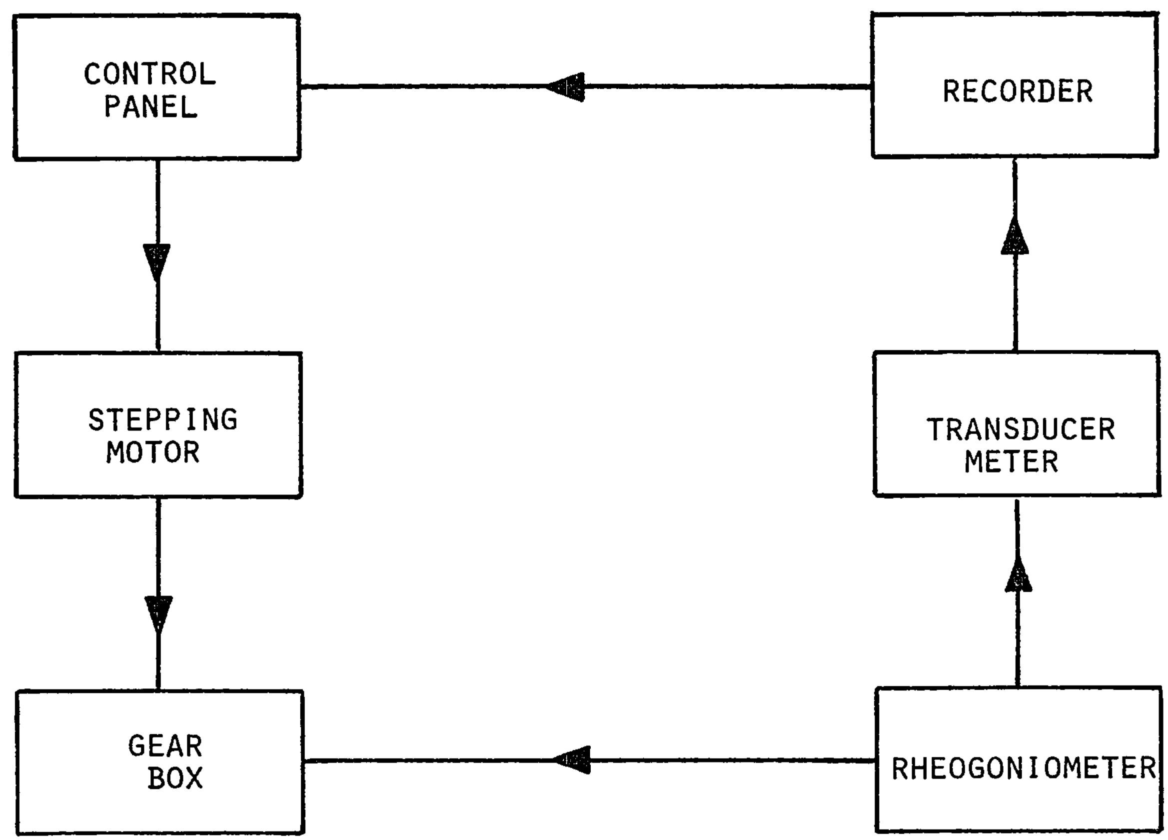

FIGURE 9: BLOCK DIAGRAM OF THE MODIFIED WEISSENBERG RHEOGONIOMETER

tions were employed as the standard for all the rheological determinations. A typical set of flow and torque-decay curves is shown in Figures 10 and 11. The smooth curve represents the actual data tracing from the X-Y recorder output. As can be seen in Figure 10, there is a slight time lag for the upcurve. These delayed responses were due to the nature of the equipment and the affected data were not incorporated into the analysis.

FIGURE 10: EXPERIMENTAL HYSTERESIS LOOP OF A BLOOD SAMPLE

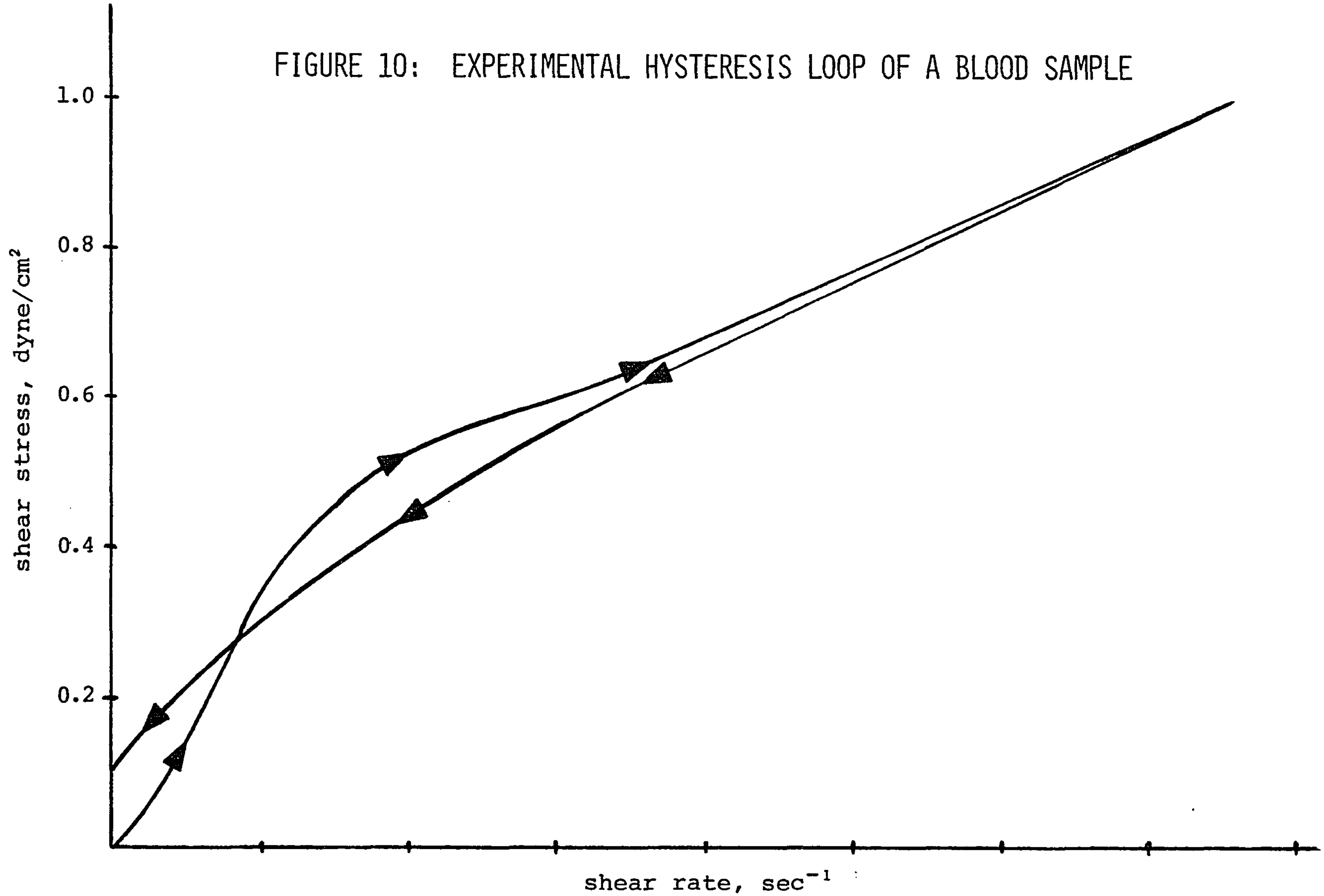

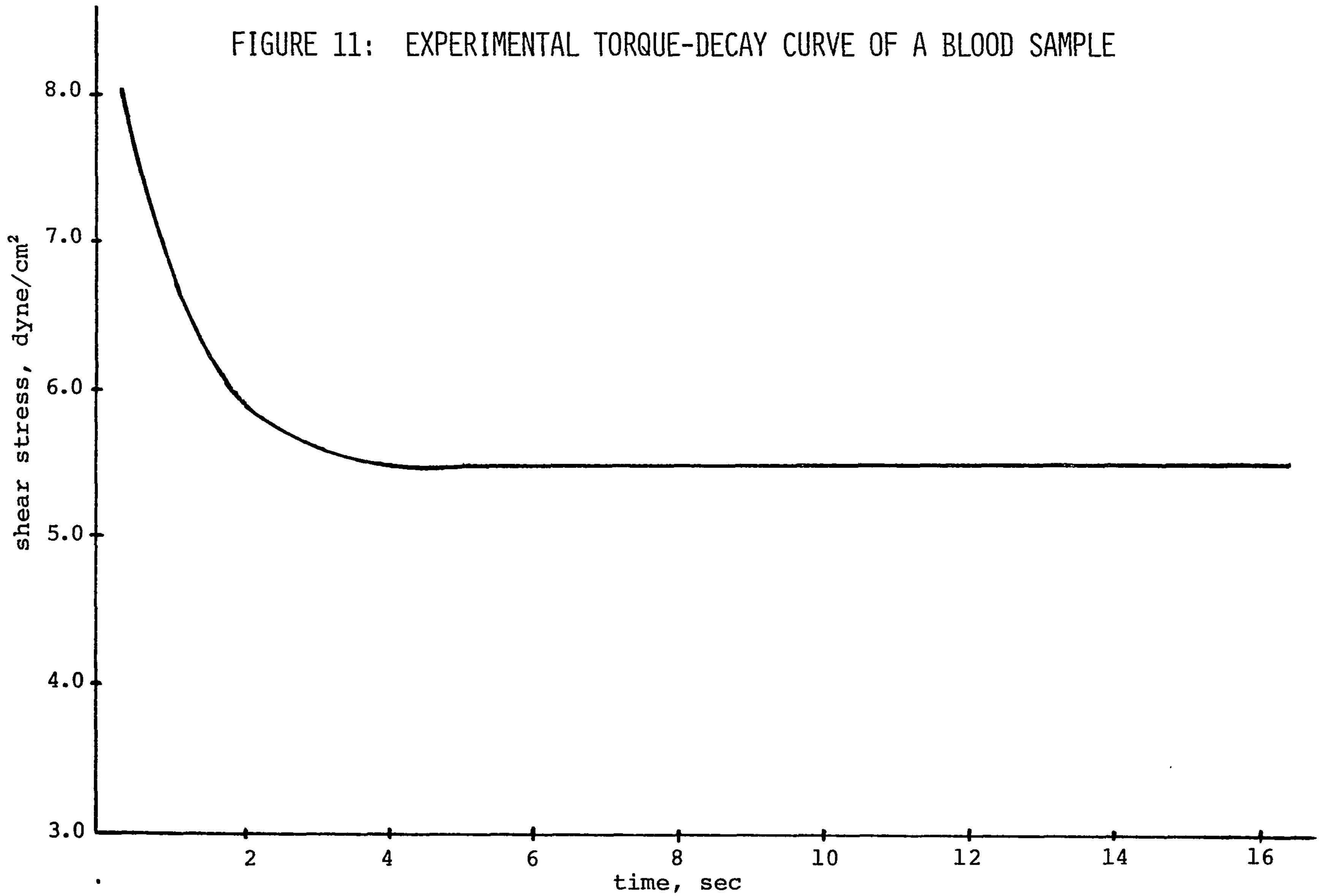

FIGURE 11: EXPERIMENTAL TORQUE-DECAY CURVE OF A BLOOD SAMPLE

APPENDIX B

PARAMETER ESTIMATION

The Huang equation for thixotropic materials contains five adjustable parameters. In order to quantitatively characterize the rheological behavior of a thixotropic material, these five parameters must be known or, at least, estimates of them must be available. Many algorithms for the least squares estimation of nonlinear parameters have used either one of two methods. The model may be expanded as a Taylor series and corrections to the parameters may be calculated at each iteration on the assumption of local linearity. Alternatively, variations of the method of a gradient search may be used. Both methods have their advantages and disadvantages. The Taylor series approach is a rapid method, but it also has the possibility of diverging from the correct solution. The gradient search method usually has excellent converging properties, but is agonizingly slow in its convergence. Marquardt (30) has developed a compromise method which he has called the maximum neighborhood method. The method performs an optimum interpolation between the Taylor series method and the gradient search. The interpolation is based upon the maximum neighborhood in which the truncated Taylor series gives an adequate representation of the nonlinear model. Marquardt's algorithm is attractive because it enables the user to incorporate either analytical or estimated partial derivatives in the linearization portion of the method.

To obtain estimates of the thixotropic parameters in the Huang rheological model, experimental shear stress versus shear rate data must be available. This data can then be regressed using the Marquardt method to estimate values for the five parameters. Although it is possible to use estimates of the partial derivatives in the Marquardt method, it is preferable to use analytic partials, if possible. Since the Huang equation takes on three distinct forms for the various sets of conditions used, a total of fifteen partial derivatives will be required. The Huang equation for the upcurve was given as

$$\tau = \tau_0 + \mu\dot{\gamma} + c_1 A\dot{\gamma}^n \exp[-(c_1\dot{\gamma}^{n+1}/\alpha(n+1)] \qquad \text{(B-1)}$$

To simplify the expressions in the partial derivatives, let

$$j = n + 1 \qquad \text{(B-2)}$$

The partial derivatives for the upcurve are as follows:

$$\partial\tau/\partial\tau_0 = 1 \qquad \text{(B-3)}$$

$$\partial\tau/\partial\mu = \dot{\gamma} \qquad \text{(B-4)}$$

$$\partial\tau/\partial c_1 = A\dot{\gamma}^n \exp[(-c_1\dot{\gamma}^j/\alpha j)][1 - (c_1\dot{\gamma}^j/\alpha j)] \qquad \text{(B-5)}$$

$$\partial\tau/\partial A = c_1\dot{\gamma}^n \exp[(-c_1\dot{\gamma}^j/\alpha j)] \qquad \text{(B-6)}$$

$$\partial\tau/\partial n = c_1 A\dot{\gamma}^n \exp[(-c_1\dot{\gamma}^j/\alpha j)][\ln(\dot{\gamma}) - (c_1\dot{\gamma}^j \ln(\dot{\gamma})/\alpha j)$$

$$+ (c_1\dot{\gamma}^j/\alpha j^2)] \quad \text{(B-7)}$$

For the downcurve, the Huang equation was given as

$$\tau = \tau_0 + \mu\dot{\gamma} + c_1 A\dot{\gamma}^n \exp[(-c_1/\alpha j)(2\dot{\gamma}_m^j - \dot{\gamma}^j)] \quad \text{(B-8)}$$

with the parameter partial derivatives being

$$\partial\tau/\partial\tau_0 = 1 \quad \text{(B-9)}$$

$$\partial\tau/\partial\mu = \dot{\gamma} \quad \text{(B-10)}$$

$$\partial\tau/\partial c_1 = A\dot{\gamma}^n \exp[(-c_1/\alpha j)(2\dot{\gamma}_m^j - \dot{\gamma}^j)]$$

$$[1 - (c_1/\alpha j)(2\dot{\gamma}_m^j - \dot{\gamma}^j)] \quad \text{(B-11)}$$

$$\partial\tau/\partial A = c_1\dot{\gamma}^n \exp[(-c_1/\alpha j)(2\dot{\gamma}_m^j - \dot{\gamma}^j)] \quad \text{(B-12)}$$

$$\partial\tau/\partial n = c_1 A\dot{\gamma}^n \exp[(-c_1/\alpha j)(2\dot{\gamma}_m^j - \dot{\gamma}^j)][\ln(\dot{\gamma}) - (c_1/\alpha j)$$

$$(2\dot{\gamma}_m^j \ln(\dot{\gamma}_m) - \dot{\gamma}^j \ln(\dot{\gamma}) + (c_1/\alpha j^2)(2\dot{\gamma}_m^j - \dot{\gamma}^j)] \quad \text{(B-13)}$$

The Huang equation for the torque-decay curve was given as

$$\tau = \tau_0 + \mu\dot{\gamma}_c + c_1 A\dot{\gamma}_c^n \exp[-c\dot{\gamma}_c^n t] \quad \text{(B-14)}$$

with the parameter partial derivatives being

$$\partial\tau/\partial\tau_0 = 1 \qquad \text{(B-15)}$$

$$\partial\tau/\partial\mu = \dot{\gamma}_c \qquad \text{(B-16)}$$

$$\partial\tau/\partial c_1 = A\dot{\gamma}_c^n \exp[1 - c_1\dot{\gamma}_c^n t] \qquad \text{(B-17)}$$

$$\partial\tau/\partial A = c_1\dot{\gamma}_c^n \exp[-c_1\dot{\gamma}_c^n t] \qquad \text{(B-18)}$$

$$\partial\tau/\partial n = c_1 A\dot{\gamma}_c^n \exp[-c_1\dot{\gamma}_c^n t][\ln(\dot{\gamma}_c)(1 - c_1\dot{\gamma}_c^n t)] \qquad \text{(B-19)}$$

The Marquardt algorithm is a conventional least squares method with the minimization function being defined as the sum of the squares of the differences of the observed and predicted values. The objective function is expressed as

$$\Phi = \sum_{i=1}^{N} [(\text{observed value})_i - (\text{predicted value})_i]^2$$

where Φ is the minimization function and N is the number of data points. The goodness of fit of the model is described by the standard error of the estimate defined as

$$\text{S.E.} = \sqrt{[\Phi/(N - \text{NPARAM})]}$$

where NPARAM is the number of adjustable parameters in the model.

A sample computer output for a typical blood sample is presented in Figure 12. The program has the capability of imposing constraints on the model parameters to minimize the occurence of objective function divergence. The program also plots the regression results using the notation of "O" for an observed data point, "P" for a predicted point, and "Y" denotes a point where both the observed and predicted points fall within the same grid squares on the plot indicating agreement between the two values. The three distinct curves displayed in the print-out are the upcurve, downcurve, and the torque-decay curve. Additionally, the observed and predicted values are tabulated along with their respective differences. The remaining column indicates the appropriate corresponding value of shear rate or time. The remaining output includes statistical, correlation, and confidence limit information that are generated by the main program.

PASSED GAMMA EPSILON TEST

NDATA = 45   NPARAM = 5   NFIXED = 0   NVAR = 2
FF = 4.000E 00   T = 2.000E 00   B = 5.000E-07   TAU = 1.000E-03

PARAMETER MINIMUMS	9.99999930E-04	9.99999930E-04	9.99999930E-04	9.99999930E-04	9.99999930E-04
PARAMETER MAXIMUMS	1.00000000E 00	1.00000000E 00	1.00000000E 03	1.00000000E 03	1.00000000E 01
(11) MODEL PARAMETERS	9.18167230E-02	7.86448710E-02	1.57895020E-01	3.75369780E-01	1.26817700E 00

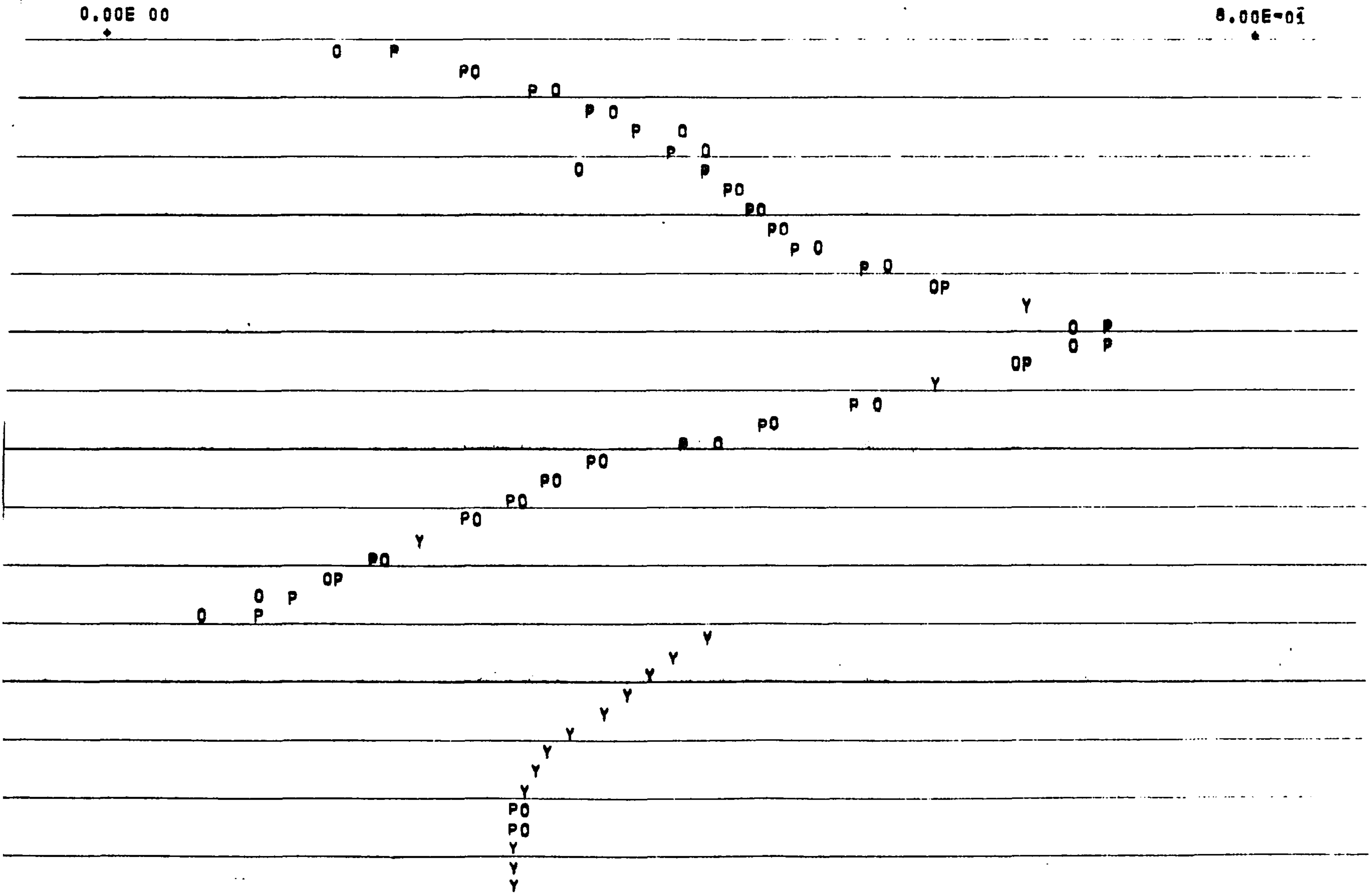

FIGURE 12: SAMPLE COMPUTER OUTPUT

PARAMETER MINIMUMS	9.99999930E-04	9.99999930E-04	9.99999930E-04	9.99999930E-04	9.99999930E-04
PARAMETER MAXIMUMS	1.00000000E 00	1.00000000E 00	1.00000000E 03	1.00000000E 03	1.00000000E 01
(11) MODEL PARAMETERS	9.18167230E-02	7.86448710E-02	1.57895020E-01	3.75369780E-01	1.26817700E 00

OBSERVED	PREDICTED	DIFFERENCE	
1.57073020E-01	1.92345440E-01	-3.52724190E-02	7.66466020E-01
2.48699000E-01	2.44684810E-01	4.01419400E-03	1.14969920E 00
3.07601980E-01	2.92572020E-01	1.50299660E-02	1.53293220E 00
3.46870000E-01	3.33416990E-01	1.34530060E-02	1.91616530E 00
3.92683020E-01	3.66126470E-01	2.65565510E-02	2.29939840E 00
4.12316970E-01	3.91193620E-01	2.11233490E-02	2.68263050E 00
3.25407020E-01	4.10407780E-01	-8.50007530E-02	3.06586360E 00
4.38495990E-01	4.26269350E-01	1.22266410E-02	3.44909660E 00
4.51586000E-01	4.41314220E-01	1.02717870E-02	3.83232970E 00
4.64675000E-01	4.57565780E-01	7.10922470E-03	4.21556280E 00
4.90854020E-01	4.76250580E-01	1.46034350E-02	4.59879580E 00
5.36666980E-01	5.22016400E-01	1.46505830E-02	5.36526200E 00
5.75935000E-01	5.76335010E-01	-4.00006770E-04	6.13172810E 00
6.34837980E-01	6.34809550E-01	2.84314150E-05	6.89819430E 00
6.67562000E-01	6.94681100E-01	-2.71191000E-02	7.66466040E 00
6.67562000E-01	6.94681100E-01	-2.71191000E-02	7.66466040E 00
6.30910990E-01	6.34333960E-01	-3.42297550E-03	6.89819430E 00
5.69391010E-01	5.74047140E-01	-4.65613600E-03	6.13172810E 00
5.30121980E-01	5.13767360E-01	1.63546200E-02	5.36526200E 00
4.58131010E-01	4.53488460E-01	4.64254610E-03	4.59879580E 00
4.18861980E-01	3.93209750E-01	2.56522290E-02	3.83232970E 00
3.40326010E-01	3.32931160E-01	7.39485020E-03	3.06586360E 00
3.07601980E-01	3.02791830E-01	4.81015440E-03	2.68263050E 00
2.87967970E-01	2.72652560E-01	1.53154130E-02	2.29939840E 00
2.48699000E-01	2.42513290E-01	6.18571040E-03	1.91616530E 00
2.15975990E-01	2.12373970E-01	3.60202780E-03	1.53293220E 00
1.89796980E-01	1.82234640E-01	7.56233930E-03	1.14969920E 00
1.50529020E-01	1.52095310E-01	-1.56629080E-03	7.66466020E-01
9.81708160E-02	1.21955990E-01	-2.37851730E-02	3.83233010E-01
5.89024980E-02	9.78445410E-02	-3.89420420E-02	7.66466250E-02
4.12316970E-01	4.14732990E-01	-2.41601460E-03	3.99999970E-01
3.90065010E-01	3.91143080E-01	-1.07806920E-03	8.00000010E-01
3.69122020E-01	3.71469670E-01	-2.34764810E-03	1.19999980E 00
3.53415010E-01	3.55062540E-01	-1.64753190E-03	1.60000030E 00
3.40326010E-01	3.41379400E-01	-1.05339280E-03	2.00000000E 00
3.14146990E-01	3.16302830E-01	-2.15584030E-03	3.00000000E 00
2.97129980E-01	3.00375220E-01	-3.24523440E-03	4.00000000E 00
2.90585990E-01	2.90258640E-01	3.27348700E-04	5.00000000E 00
2.87967970E-01	2.83832960E-01	4.13501260E-03	6.00000000E 00
2.84040980E-01	2.79751650E-01	4.28932900E-03	7.00000000E 00
2.81323010E-01	2.77159390E-01	4.16362280E-03	8.00000000E 00
2.78805010E-01	2.74467110E-01	4.33790680E-03	1.00000000E 01
2.77495980E-01	2.73380930E-01	4.11504500E-03	1.20000000E 01
2.77495980E-01	2.72942780E-01	4.55319880E-03	1.40000000E 01
2.77495980E-01	2.72765990E-01	4.72998610E-03	1.60000000E 01

PHI S E LAMBDA ANALYTIC PARTIALS USED

PTP INVERSE

1	1.25223210E-01	-2.37996500E-02	-9.65731730E-02	-4.27690200E-01	1.45309440E 00
2	-2.37996390E-02	6.99704880E-03	2.62227200E-02	2.85168690E-02	-1.47594030E-01
3	-9.65728160E-02	2.62227280E-02	2.51293560E 00	3.88936990E-01	-1.77786860E 01
4	-4.27690200E-01	2.85168920E-02	3.88937950E-01	5.25274270E 00	-1.89258420E 01
5	1.45309350E 00	-1.47594210E-01	-1.77787010E 01	-1.89258420E 01	2.12283990E 02

PARAMETER CORRELATION MATRIX

1	1.0000	-0.8040	-0.1722	-0.5273	0.2818
2	-0.8040	1.0000	0.1978	0.1487	-0.1211
3	-0.1722	0.1978	1.0000	0.1071	-0.7698
4	-0.5273	0.1487	0.1071	1.0000	-0.5668
5	0.2818	-0.1211	-0.7698	-0.5668	1.0000

PARA	STD ERROR	ONE-PARAMETER LOWER	ONE-PARAMETER UPPER	SUPPORT PLANE LOWER	SUPPORT PLANE UPPER
1	7.05464180E-03	7.77074090E-02	1.05925970E-01	6.02674110E-02	1.23365990E-01
2	1.66759220E-03	7.53096340E-02	8.19800490E-02	7.11871380E-02	8.61025450E-02
3	3.16026350E-02	9.46897860E-02	2.21100270E-01	1.65637730E-02	2.99226280E-01
4	4.56904760E-02	2.83988830E-01	4.66750740E-01	1.71035820E-01	5.79703740E-01
5	2.90463260E-01	6.87250490E-01	1.84910290E 00	-3.08132170E-02	2.56716720E 00

NONLINEAR CONFIDENCE LIMITS PHI CRITICAL = 2.38460600E-02

PARA	LOWER B	LOWER PHI	UPPER B	UPPER PHI
1	7.85266750E-02	2.38458060E-02	1.05107420E-01	2.38460220E-02
2	7.49616020E-02	2.38456500E-02	8.23283790E-02	2.38461230E-02
3	9.51019520E-02	2.47384710E-02	2.41203900E-01	2.40294330E-02
4	2.74255210E-01	2.38458880E-02	4.76487570E-01	2.38460150E-02
5	7.28090820E-01	2.37029040E-02	1.80285350E 00	2.38622570E-02

END OF SAMPLE #91 ABNORMAL CAUCASIAN MALE,AGE=54

APPENDIX C

NOMENCLATURE

a = angular acceleration of outer cylinder

A = Huang equation parameter

A_1 = constant defined by equation (4-26a)

A_2 = constant defined by equation (4-26b)

C_1 = Huang equation parameter

C = integration constant

C_v = vascular conductance

d = diameter

D = integration constant

E = series constant defined by equation (4-28)

F = function defined by equation (4-22)

g = gravitational force per unit mass

G = function defined by equation (4-57)

i = index

j = constant defined by equation (B-2)

J_1 = first order Bessel function of the first kind

k = consistency index

k_0 = Casson equation parameter

k_1 = Casson equation parameter

L = length

m = flow behavior index

n = Huang equation parameter

NPARAM = number of adjustable parameters

N_{HF} = Huang-Fabisiak number

N_{Re} = Reynolds number

p = static pressure

P = probability parameter

PRU = peripheral resistance unit

Q = volumetric flow rate

r = radius

R = radius of outer cylinder

R_v = vascular resistance

R_1, R_2, R_3, R_4 = double Couette radii

S.E. = standard error of estimate

t = time

t_1 = time for shear rate to reach its maximum value

t_2 = total time for ramp function

T = total torque

T_i = torque exerted on inner cylinder

T_o = torque exerted on outer cylinder

T_1, T_2 = torque functions defined by equation (4-36)

T^* = dimensionless torque

v = velocity

Y_1 = first order Bessel function of second kind

Z = combination Bessel function

α = proportionality constant

β = eigenvalue

$\dot{\gamma}$ = shear rate

$\dot{\gamma}_c$ = constant value of shear rate

$\dot{\gamma}_m$ = maximum value of shear rate

ζ = constant defined by equation (4-25c)

η = apparent viscosity

η_s = steady-state viscosity

θ = angular coordinate

κ = concentric cylinder radius ratio

λ = regression constant

μ = Newtonian viscosity

ξ = dummy variable

ρ = fluid density

σ = dimensionless time

τ = shear stress

τ_0 = yield stress

Φ = minimization function

ω = rotational speed

Ω = angular velocity

REFERENCES

1. Copley, A. L., Science, 94, 543 (1941).

2. Copley, A. L., J. Colloid Sci., 7, 323 (1952).

3. Dintenfass, L., Circulation Res., 11, 233 (1962).

4. Dintenfass, L., "Blood Microrheology: Viscosity Factors in Blood Flow, Ischaemic and Thrombosis", Butterworths, London (1971).

5. Dintenfass, L., "Rheology of Blood in Diagnostic and Preventive Medicine: An Introduction to Clinical Haemorheology", Butterworths, London (1976).

6. Aronson, H. B., Magora, F. and Schenker, J. G., Am. J. Obst. and Gyn., 110, 997 (1971).

7. Stormer, B., Horsch, R., Kleinschmidt, F., Loose, D., Bruster, H. and Kremer, K., J. Cardiovascular Surgery, 15, 577 (1974).

8. Chmiel, H., Biorheology, 11, 87 (1974).

9. Cokelete, G. R., Merril, E. W., Gilliland, E. R., Shin, H., Britten, A. and Wells, R. E., Trans. Soc. Rheo., 7, 303 (1963).

10. Casson, N., "Rheology of Disperse Systems", (Edited by Mills, D. C.) 84-102, Pergamon Press, Oxford (1959).

11. Copley, A. L., Krchma, L. C. and Whitney, M. E., J. General Physiol., 26, 49 (1942).

12. Dintenfass, L., Kolloidzeitschrift, 180, 160 (1962).

13. Huang, C. R., Copley, A. L. and King, R. G., Biorheology, 10, 23 (1973).

14. Huang, C. R., Siskovic, N., Robertson, R. W. J., Wang, H. H. and Orosz, P. J., Biorheology, 9, 155 (1972).

15. Huang, C. R., Siskovic, N., Robertson, R. W. J., Fabisiak, W., Smithberg, E. H. and Copley, A. L., Biorheology, 12, 279 (1975).

16. Huang, C. R. and Fabisiak, W., Thrombosis Research, 8, Supplement II, 1 (1976).

17. Guyton, A. C., "Textbook of Medical Physiology", 5th Edition, W. B. Saunders Co., Philadelphia (1976).

18. Bird, R. B., Stewart, W. E. and Lightfoot, E. N., "Transport Phenomena", John Wiley & Sons, New York (1960).

19. Skelland, A. H. F., "Non-Newtonian Flow and Heat Transfer", John Wiley & Sons, New York (1967).

20. Orosz, P. J., "Characterization of Thixotropic Materials and Modification of the Weissenberg Rheogoniometer", Eng. Sc. D. Dissertation in Chemical Engineering, Newark College of Engineering, Newark, New Jersey (1974).

21. Huang, C. R., Chem. Eng. Journal, 3, 100 (1972).

22. Huang, C. R., Fabisiak, W. and Polston, N. L., Proceedings of the Seventh International Congress on Rheology, 238 (1976).

23. Huang, C. R. and Fabisiak, W., AIChE Symposium Series, 182, Vol. 74, 19 (1978).

24. Sinusas, R. R., "Design and Analysis of an Instrument System for Rheological Testing of Whole Blood Samples", Eng. Sc. D. Dissertation in Mechanical Engineering, Newark College of Engineering, Newark, New Jersey (1974).

25. Bird, R. B. and Curtiss, C. F., Chem. Eng. Sci., 11, 108 (1959).

26. Bureau, M., Healy, J. C., Bourgoin, D. and Joly, M., Paper 12-4, Proceedings of the Third International Congress on Biorheology, (1978).

27. Huang, C. R., Su, J. A., Fabisiak, W., Anadhi, C., Engler, P. E., Geissler, B., Cohn, J. D. and Redo, S. F., Paper 17.1, 31st Annual Conference on Engineering in Medicine and Biology, (1978).

28. Fabisiak, W. and Huang, C. R., Paper 12-5, Proceedings of the Third International Congress on Biorheology, (1978).

29. Churchill, R. V., "Operational Mathematics", 2nd Ed., McGraw-Hill, New York (1958).

30. Marquardt, D. W., J. Soc. Ind. Appl. Math., 11, 431 (1963).

31. Kreiger, I. M. and Maron, S. H., J. Appl. Phys., 23, 147 (1952).

32. Kreiger, I. M. and Elrod, H., J. Appl. Phys., 24, 134 (1953).

33. Kreiger, I. M., Trans. Soc. Rheol., 12, 5 (1968).

34. Benis, A. M., Usami, S. and Chien, S., Biorheology, 8, 65 (1971).

35. Huang, C. R., Trans. Soc. Rheol., 15, 25 (1971).